ČVUT v Praze, Fakulta strojní, Ústav strojírenské technologie, Technická 4, Praha 6, 166 07, Česká republika
T 224 352 628 E 12133@fs.cvut.cz W u12133.fs.cvut.cz

FAKULTA STROJNÍ ČVUT V PRAZE

ÚSTAV STROJÍRENSKÉ TECHNOLOGIE
TV SL SV PÚ SP

Test report no. 12133_05_2026_LK

Analysis of bolt welds

Compiler:

CTU in Prague, Faculty of Mechanical Engineering
Institute of Mechanical Engineering Technology
Technická 4
160 00, Prague 6
Registration number: 68407700

Contact person: Assoc. Ing. Ladislav Kolařík, Ph.D., IWE

Customer:
PROWELD STUD WELDING s.r.o.
Štěpaňákova 6
710 00, Ostrava
Registration number: 08935904

Contact person: Ing. David Pospíšil, IWE

Date of preparation: 26.03.2026
Number of pages: 4 3
Number of attachments: 0
Report prepared by: doc. Ing. Ladislav Kolařík, Ph.D., doc. Ing. Marie Kolaříková, Ph.D., prof. Dr. Ing. Antonín Kříž

ČVUT v Praze, Fakulta strojní, Ústav strojírenské technologie, Technická 4, Praha 6, 166 07, Česká republika
T 224 352 628 E 12133@fs.cvut.cz W u12133.fs.cvut.cz

Subject of testing – type, kind and number of samples:

A test sample containing 5 welded joints of bolts with a diameter of M12 made of material Wr.N. 1.4541, welded on a plate made of material S355, was submitted.

Fig. No. 1. – Supplied test sample with welded joints

Description of the tests performed:
Samples were taken from the test piece for metallographic analysis. Macro and microstructure tests were performed and the microhardness HV0.1 was measured on the cut sections and electron analyses were performed.

Metallographic examination of micro and macrostructure

Test equipment:	preparation – Labotom 3 cutting saw (Struers), CitoPress 1 press (Struers), Phoenix Beta metallographic grinder/polisher with automatic Vector head (Buehler)
Evaluation:	Axio Observer Dm1 metallographic microscope (Zeiss)
Etchant:	Nital 2%
Test performed by:	doc. Ing. Marie Kolaříková, Ph.D., IWE

Microhardness test

Testing equipment: hardness tester ATM Qness 60 A + EVO with SW Qpix Control2
The microhardness test HV0.1 (loading time 10s) was performed in accordance with EN ISO 6507-1, on Cross section of the welded joint, in accordance with EN ISO 9015-2
The test was performed by: doc. Ing. Ladislav Kolařík, Ph.D., IWE

SEM – Scanning Electron Microscopy

Testing equipment: VEGA 3 TESCAN electron microscope
Test performed by: Prof. Dr. Ing. Antonín Kříž, IWE

ČVUT v Praze, Fakulta strojní, Ústav strojírenské technologie, Technická 4, Praha 6, 166 07, Česká republika
T 224 352 628 E 12133@fs.cvut.cz W u12133.fs.cvut.cz

Test Results:

Macrostructure Test

Figures 2 to 6 show the macrostructures of the weld joints of samples 1 to 5.

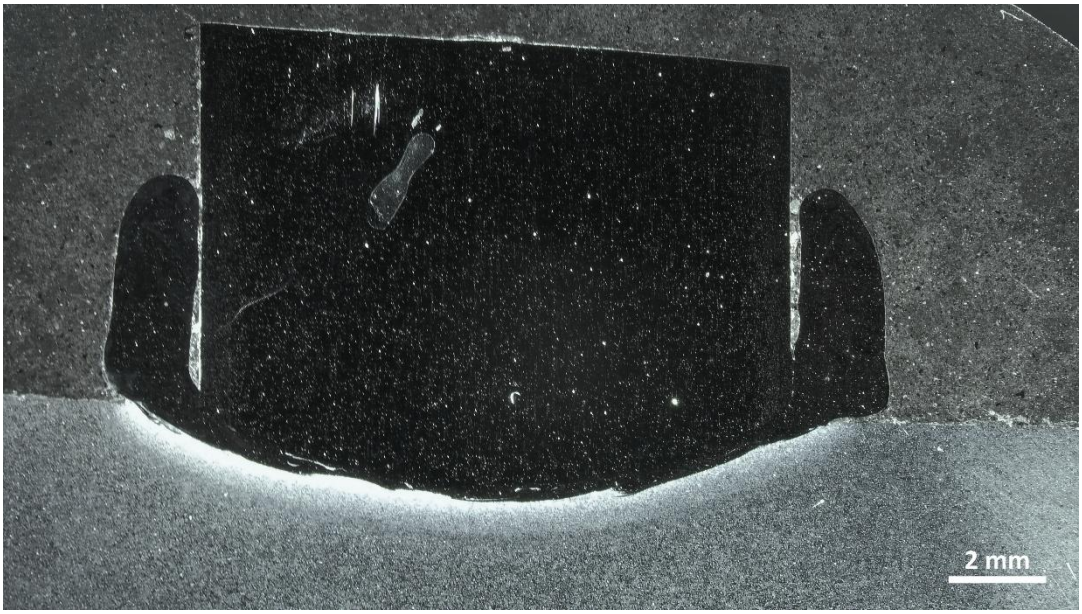

Fig. 2 – Macrostructure of the welded joint No. 1

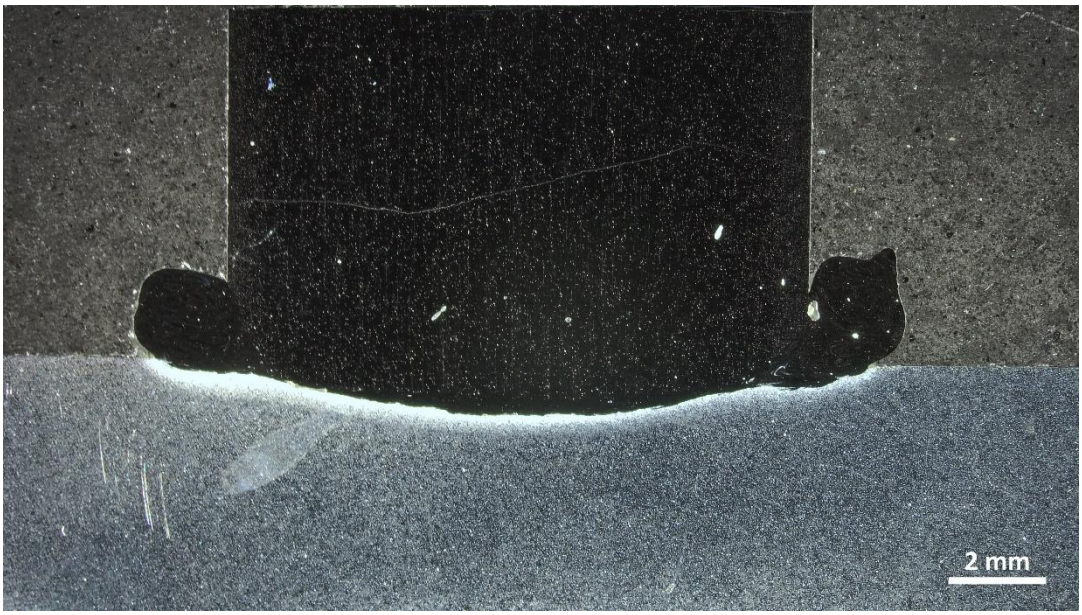

Fig. 3 – Macrostructure of the welded joint No. 2

ČVUT v Praze, Fakulta strojní, Ústav strojírenské technologie, Technická 4, Praha 6, 166 07, Česká republika
T 224 352 628 E 12133@fs.cvut.cz W u12133.fs.cvut.cz

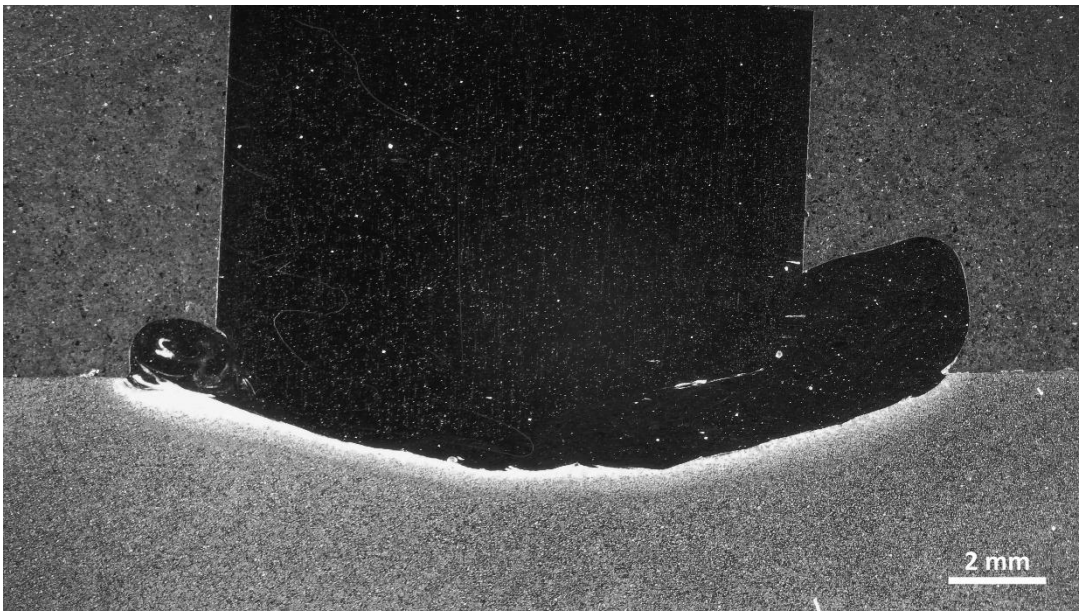

Fig. 4 – Macrostructure of the welded joint No. 3

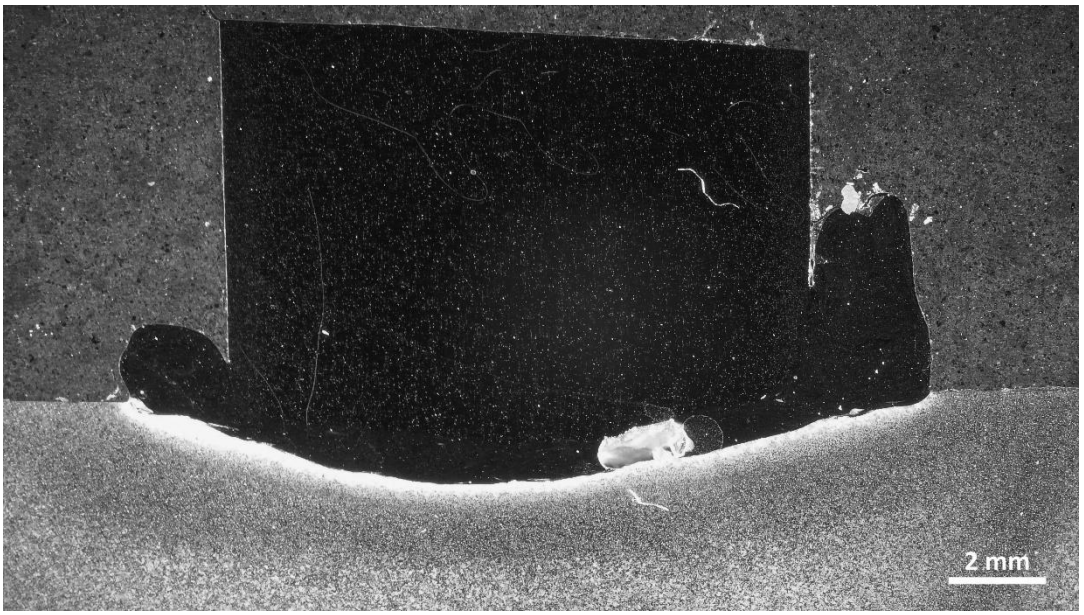

Fig. 5 – Macrostructure of the welded joint No. 4

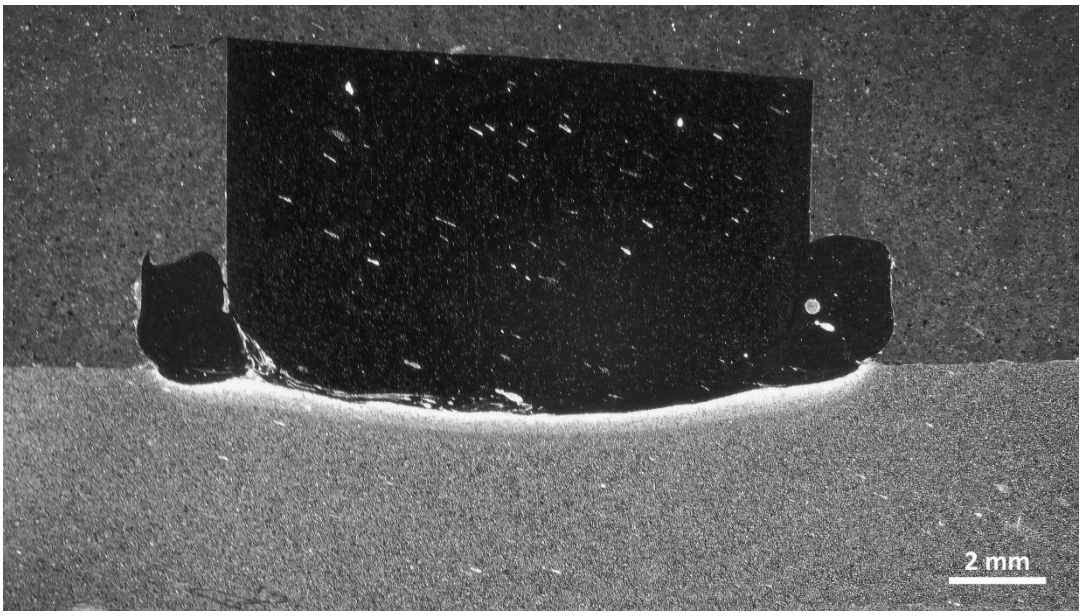

Fig. 6 – Macrostructure of the welded joint No. 5

Microstructure Test

Figures 7 to 16 show the microstructures of the weld joints of samples 1 to 5.

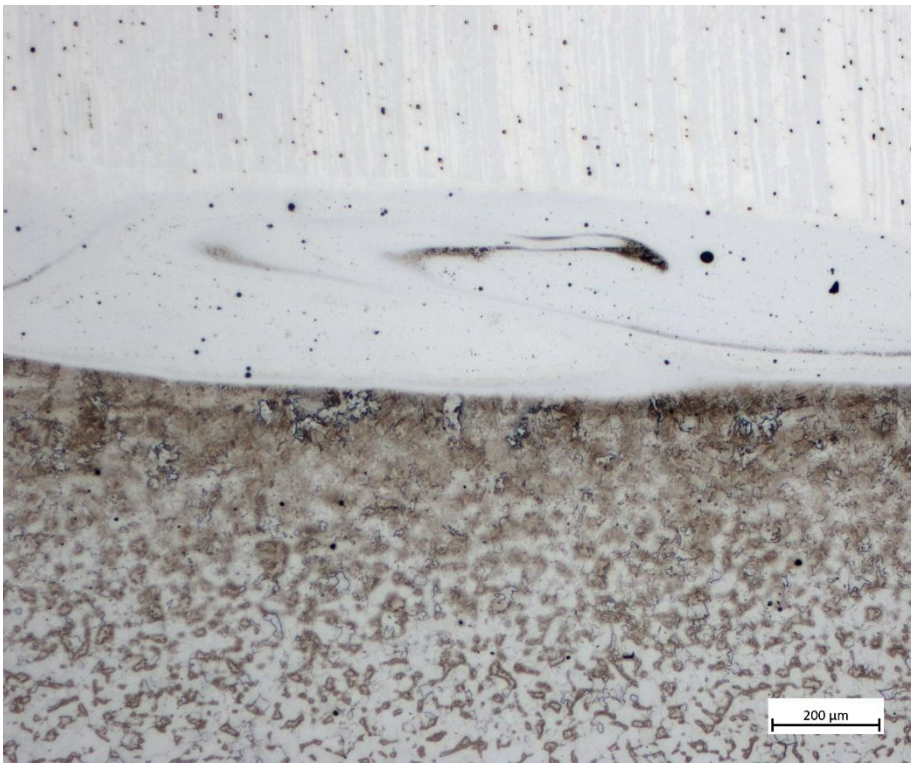

Fig. 7 – Detail of the microstructure of the welded joint No. 1 – magnification 50x

(transition between the bolt - upper part of the picture and the base plate - lower part of the picture)

ČVUT v Praze, Fakulta strojní, Ústav strojírenské technologie, Technická 4, Praha 6, 166 07, Česká republika
T 224 352 628 E 12133@fs.cvut.cz W u12133.fs.cvut.cz

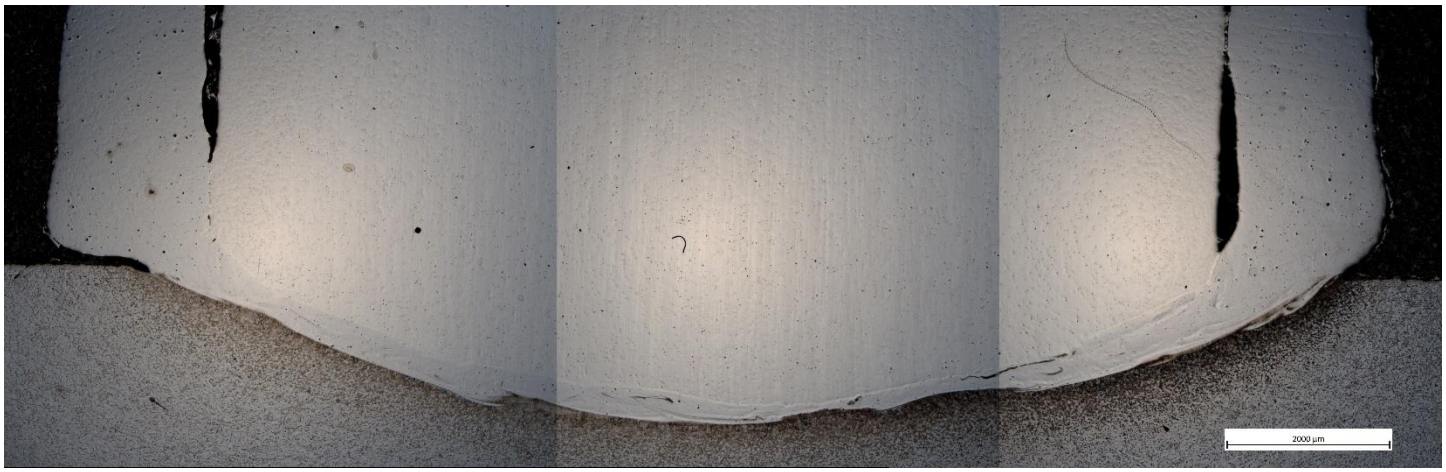

Fig. 8 – Microstructure of the entire weld joint No. 1 – magnification 25x

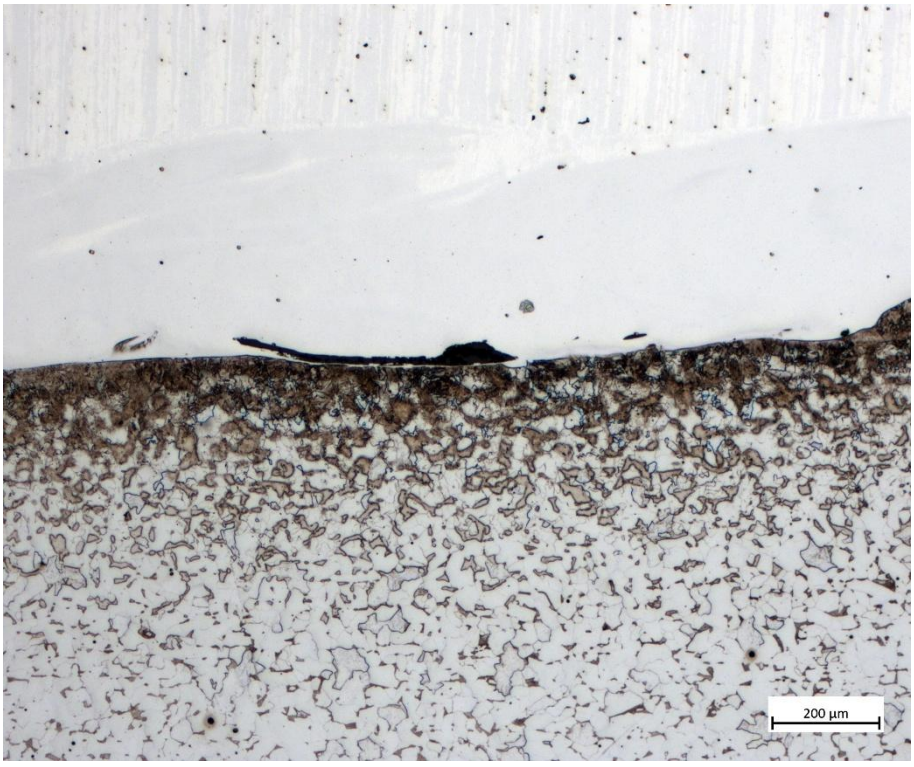

Fig. 9 – Detail of the microstructure of the welded joint No. 2 – magnification 50x

(transition between the bolt - upper part of the picture and the base plate - lower part of the picture)

Fig. 10 – Microstructure of the entire weld joint No. 2 – magnification 25x

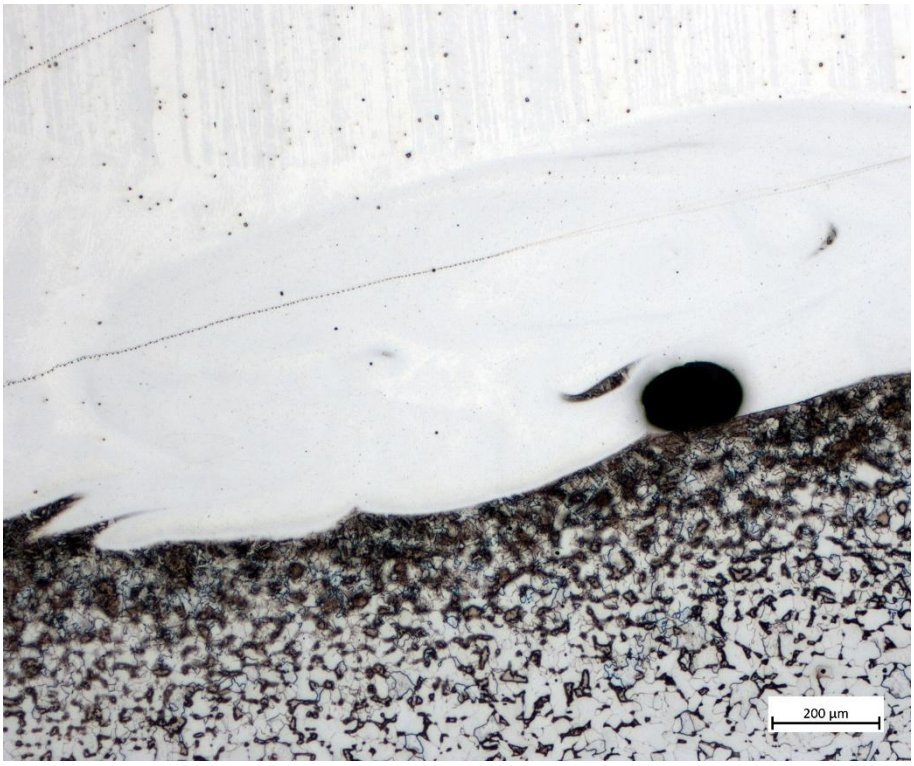

Fig. 11 – Detail of the microstructure of the welded joint No. 3 – magnification 50x

(transition between the bolt - upper part of the picture and the base plate - lower part of the picture)

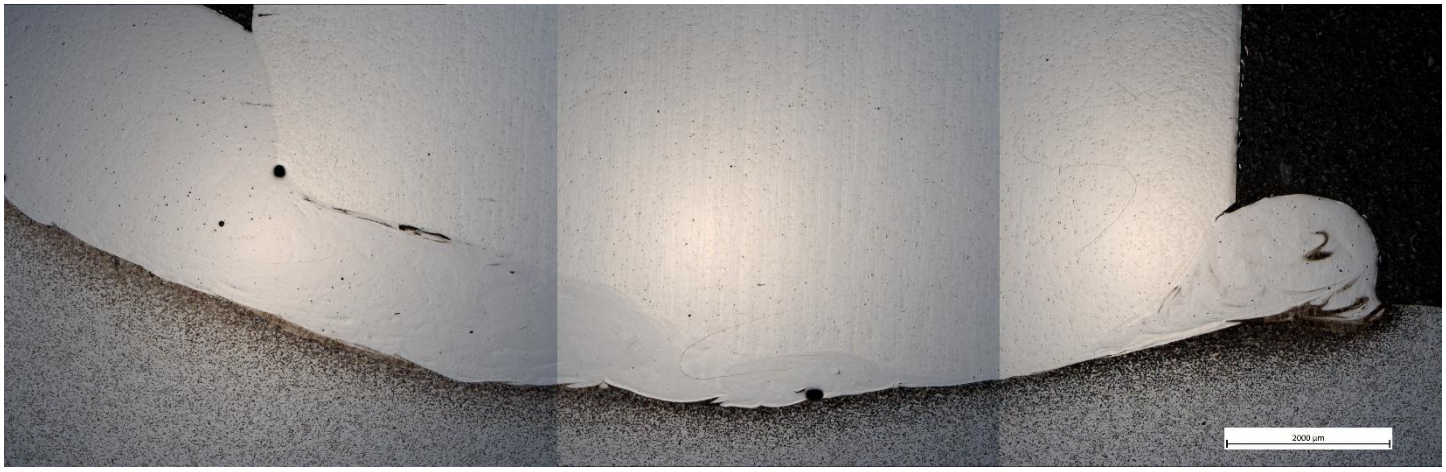

Fig. 12 – Microstructure of the entire weld joint No. 3 – magnification 25x

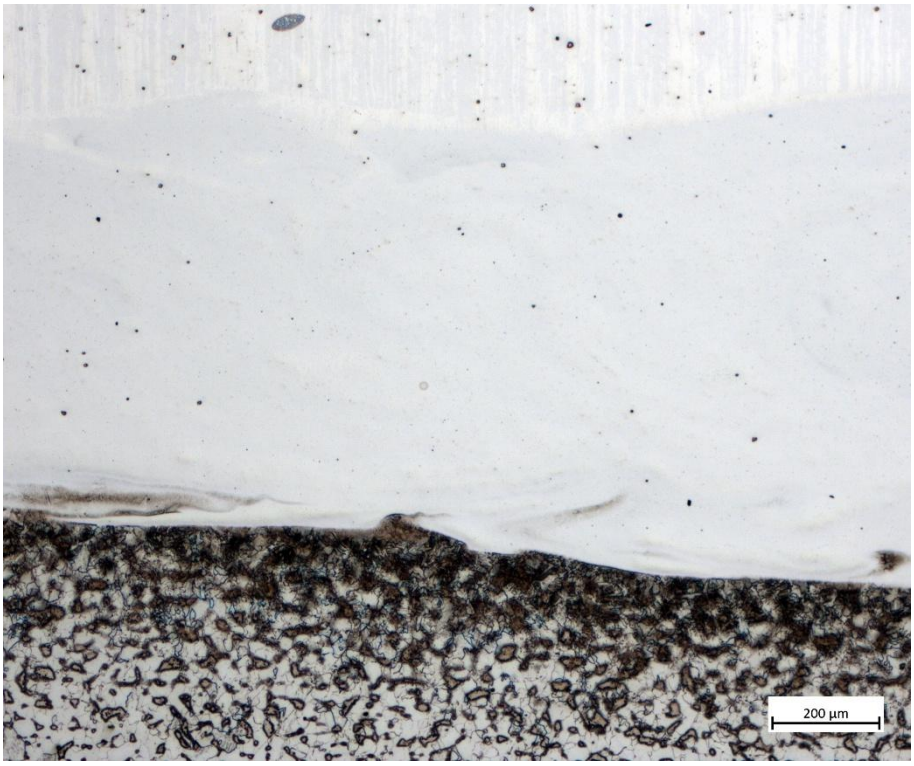

Fig. 13 – Detail of the microstructure of the welded joint No. 4 – magnification 50x

(transition between the bolt - upper part of the picture and the base plate - lower part of the picture)

Fig. 14 – Microstructure of the entire weld joint No. 4 – magnification 25x

Fig. 15 – Detail of the microstructure of the welded joint No. 5 – magnification 50x

(transition between the bolt - upper part of the picture and the base plate - lower part of the picture)

Fig. 16 – Microstructure of the entire weld joint No. 5 – magnification 25x

Fig. 17 – Microstructure of the end part of the bolt (before welding) – magnification 25x

Microhardness test

The microhardness HV0.1 was measured in several areas, as recommended by the standard for a butt T joint. The measured areas and the number of indentations in each area are indicated in Figure 18.

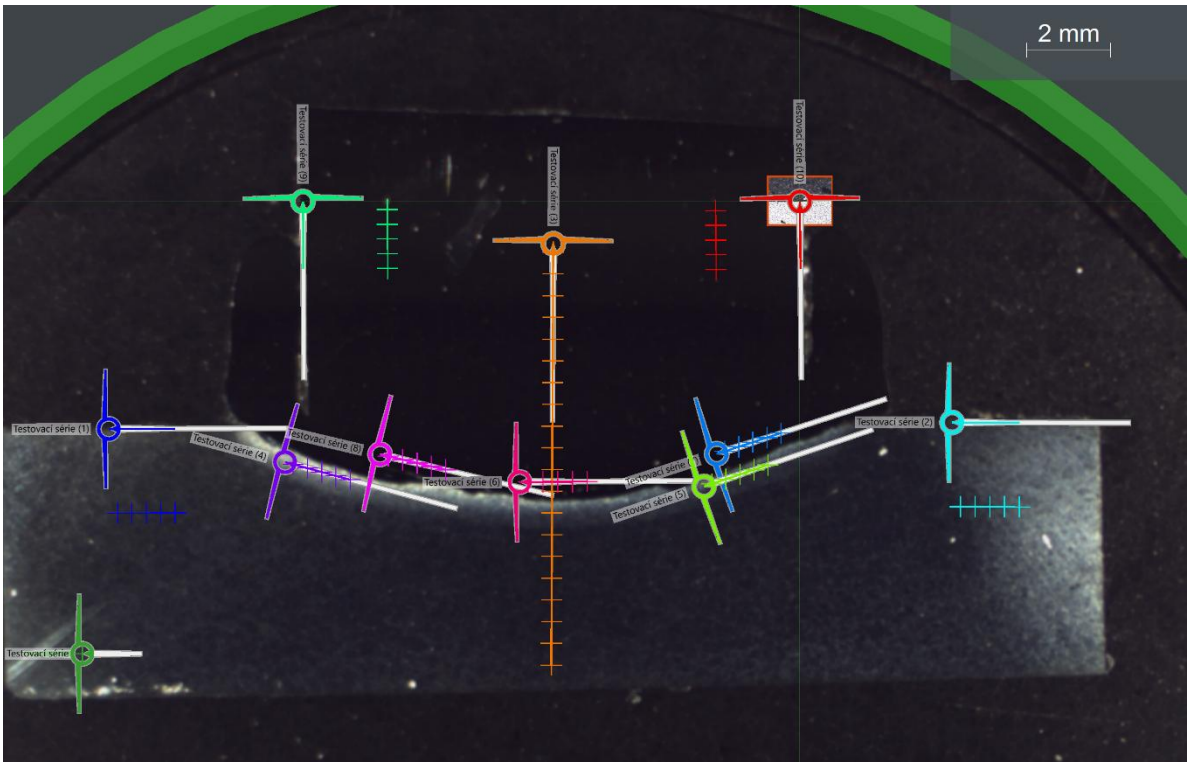

Fig. 18 – Overall view of the measured areas and the location of the individual indents during microhardness testing (location TS = test series 1 to 10)

Figures 19 to 22 show the marking of individual indents in the measured areas.

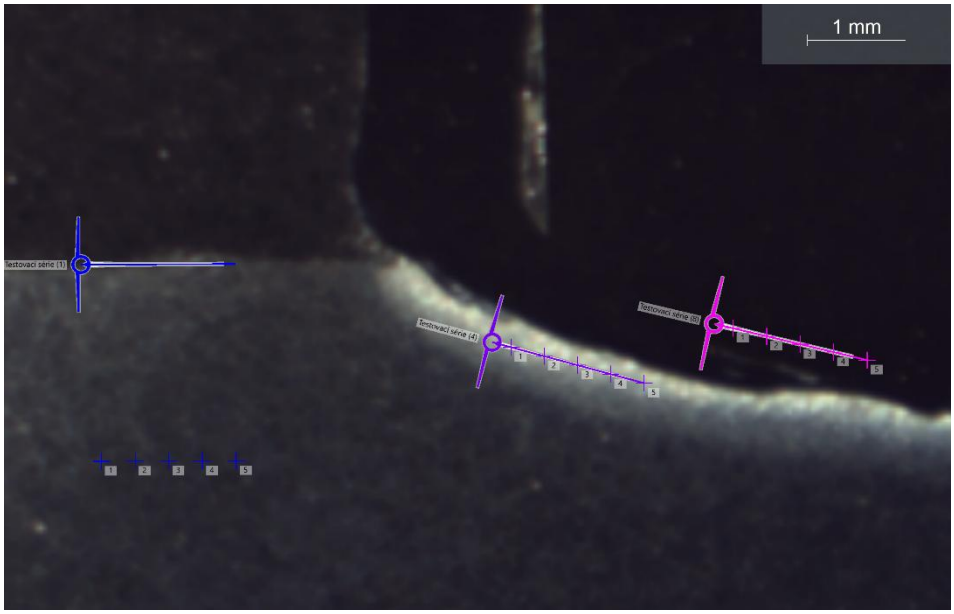

Fig. 19 – Display of the number and order of injections in a test series TS1, TS4 and TS8

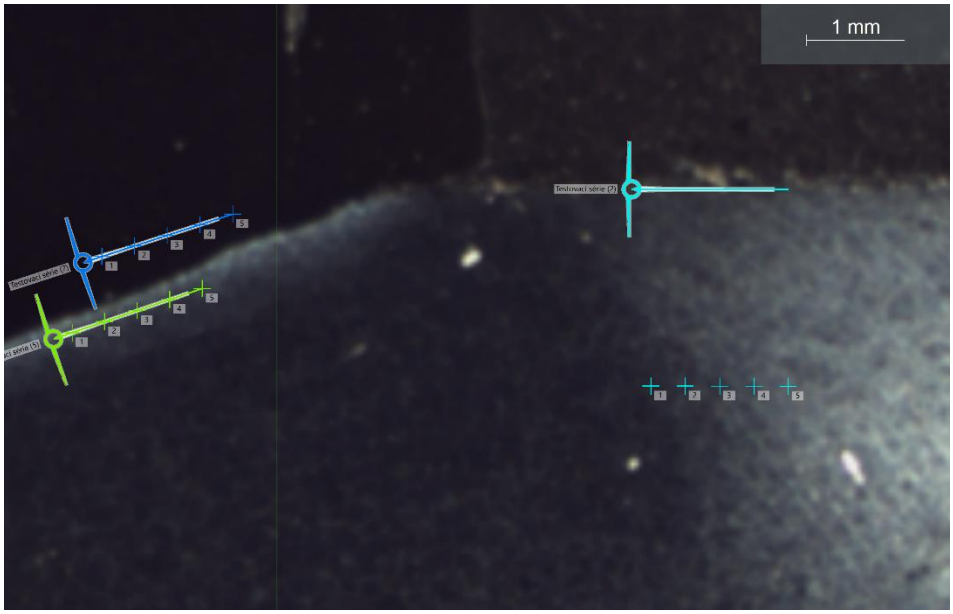

Fig. 20 – Display of the number and order of injections in a test series TS2, TS5 and TS7

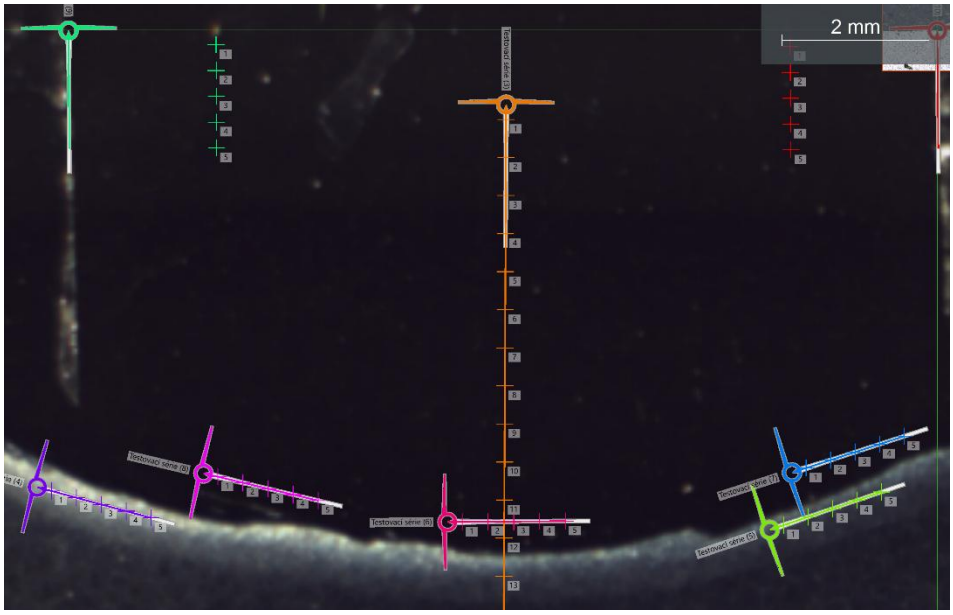

Fig. 21 – Display of the number and order of injections in a test seriesTS3, TS6 and TS9, TS10

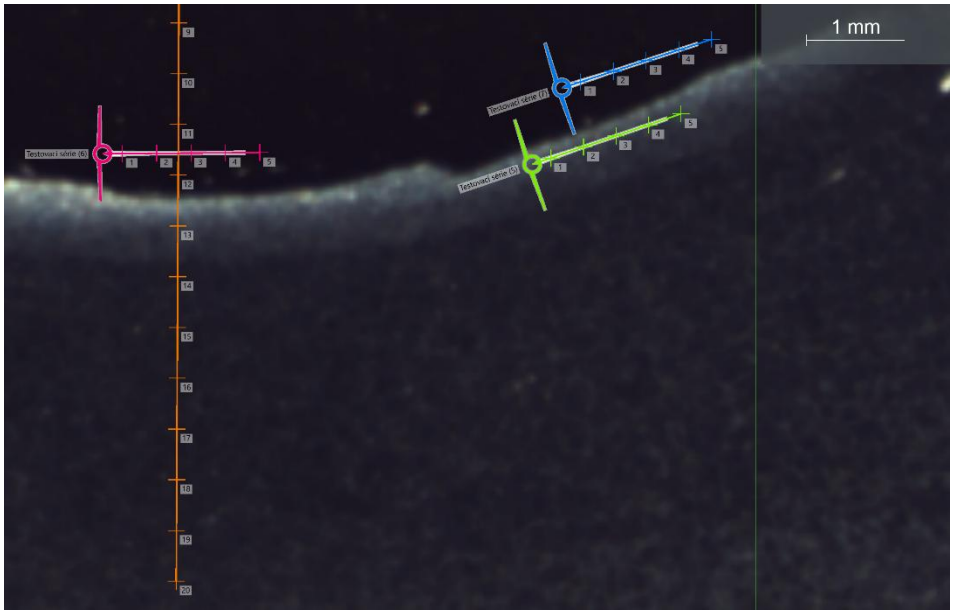

Fig. 22 – Display of the number and order of injections in a test seriesTS3, TS6 (TS5, TS7)

Note:
TS1 = Base material of the base plate (measured on the left side of the weld) – 5 punctures, distance between punctures 0.35 mm
TS2 = Base material of the base plate (measured on the right side of the weld) – 5 punctures, distance between punctures 0.35 mm
TS3 = Vertically measured transition across all zones of the weld (20 punctures, distance between punctures 0.5 mm)
TS4 = Heat affected zone (measured on the left side of the weld) – 5 punctures, distance between punctures 0.35 mm
TS5 = Heat affected zone (measured on the right side of the weld) – 5 punctures, distance between punctures 0.35 mm
TS6 = Weld metal (measured in the middle of the weld) – 5 punctures, distance between punctures 0.35 mm
TS7 = Weld metal (measured to the right of the center joint) – 5 punctures, distance between punctures 0.35 mm
TS8 = Weld metal (measured left of joint center) – 5 punctures, distance between punctures 0.35 mm
TS9 = Stud base material (measured vertically left of joint center) – 5 punctures, distance between punctures 0.35 mm
TS10 = Stud base material (measured vertically right of joint center) – 5 punctures, distance between punctures 0.35 mm

Tab. 1 – No. of SampleHV0,1

No. of Sample		TS1 (ZM)	TS2 (ZM)	TS4 (TOO)	TS5 (TOO)	TS6 (SK)	TS7 (SK)	TS8 (SK)	TS9 (ZM-Stud)	TS10 (ZM-Stud)
Sample 1	1	151	164	233	238	223	231	231	324	329
	2	148	158	237	392	233	224	233	318	316
	3	132	171	218	214	234	235	228	313	313
	4	145	169	250	216	241	222	234	320	314
	5	151	170	314	230	220	255	233	295	305
Average Vz1		144	166,4	250,5	258	230,2	233,4	231,8	311,5	315,4
Sample 2	1	141	131	240	255	239	441	378	284	306
	2	164	134	273	266	393	418	311	288	300
	3	155	139	286	243	360	390	240	297	310
	4	149	134	369	243	375	381	246	305	302
	5	152	122	212	203	342	403	425	300	307
Average Vz2		152,2	132	292	241,75	341,8	406,6	320	294,8	305
Sample 3	1	130	161	242	235	184	230	406	292	293
	2	141	135	214	201	378	215	398	290	287
	3	128	141	231	229	290	213	390	302	295
	4	138	146	218	223	197	218	418	300	310
	5	128	132	220	265	198	299	427	298	287

Average Vz3		133	143	225	219,67	249,4	235	407,8	296,4	294,4
Sample 4	1	132	166	339	217	457	426	450	312	311
	2	131	161	361	253	376	405	404	318	315
	3	132	170	335	296	212	415	441	310	322
	4	148	139	269	215	255	430	396	297	315
	5	153	154	251	233	429	442	396	314	318
Average Vz4		139,2	158	314,33	242,8	345,8	423,6	422,75	310,2	316,2
Sample 5	1	126	132	267	234	469	446	233	290	293
	2	128	134	188	223	415	440	225	293	306
	3	136	123	214	278	460	440	413	280	297
	4	130	128	229	227	380	431	220	308	298
	5	128	133	214	290	437	444	345	292	308
Average Vz5		129,6	130	220,75	246,33	432,2	440,2	300,75	292,6	300,4

Tab. 2 – Microhardness measurement resultsHV0,1 (TS3)

NO. vz	1	2	3	4	5	6	7	8	9	10	11	12	13	14	15	16	17	18	19	20
VZ1	298	290	283	293	280	284	277	280	280	284	261	338	223	210	177	181	166	171	161	158
VZ2	302	265	273	293	279	294	290	295	283	282	322	236	153	157	161	151	148	129	139	142
VZ3	278	278	291	270	270	283	269	279	281	281	280	256	240	213	406	194	160	159	157	160
VZ4	293	268	271	271	282	282	288	283	294	290	291	259	246	316	234	176	177	165	168	152
VZ5	289	281	271	275	279	294	288	293	297	277	273	411	253	166	157	163	152	156	154	141

SEM (Scanning Electron Microscopy) Analysis

Samples created for microstructure testing were used for electron analysis.

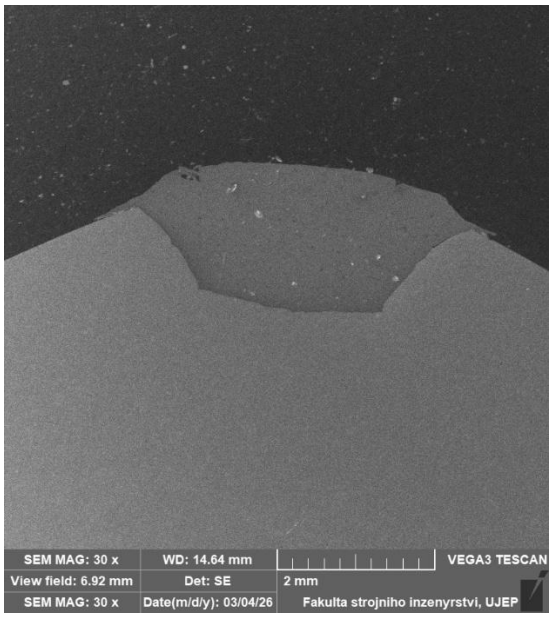

Fig. No. 23 – Stud tip, EDS analysis was performed on the contact point – this is a different Stud, however, it declares that there is an aluminum alloy ball on the tip of the Studs

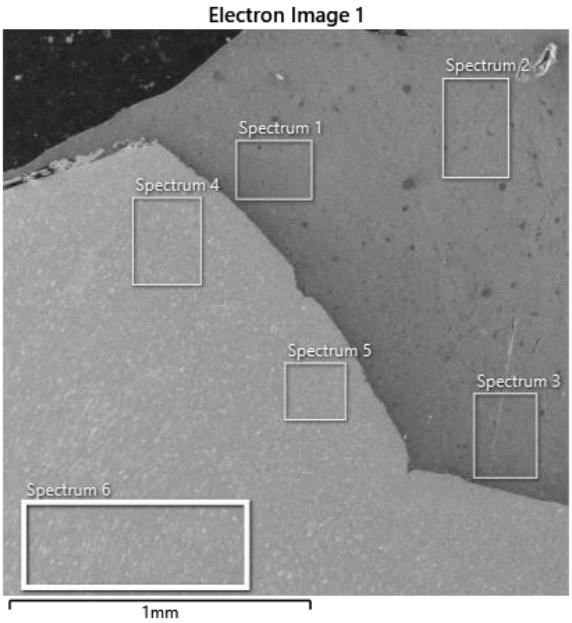

Fig. No. 24 – Areas in which EDS analysis was carried out: spectrum 1 – 98,3 % Al; 1,7 % Si; spectrum 2 – 97,3 % Al; 2,7 % Si; spectrum 3 – 97,5 % Al; 2,5 % Si; spectrum 4 – 99,5 % Fe; 0,5 % Mn; spectrum 5 – 99,5 % Fe; 0,5 % Mn; spectrum 6 – 99,6 % Fe; 0,4 % Mn.

The tip of the "ball" is an alloy of aluminum and silicon, as will be captured by further EDS analyses of individual welds, thanks to this tip, aluminum (Al-Si alloy) will also be present in the weld area. The "body" of the Stud used is made of low-carbon steel. The following Studs are made of stainless steel Wr.N. 1.4541. These are chemically different Studs (higher concentrations of Cr and Ni). Another significant difference is in thermal conductivity. Structural steel has a thermal conductivity of λ = 60; stainless steel 10; aluminum 220 [W/mK]. [Data source] GLÜCK, B.: Heizwasser Netze, VEB Verlag für Bauwesen Berlin. Berlin 1985.

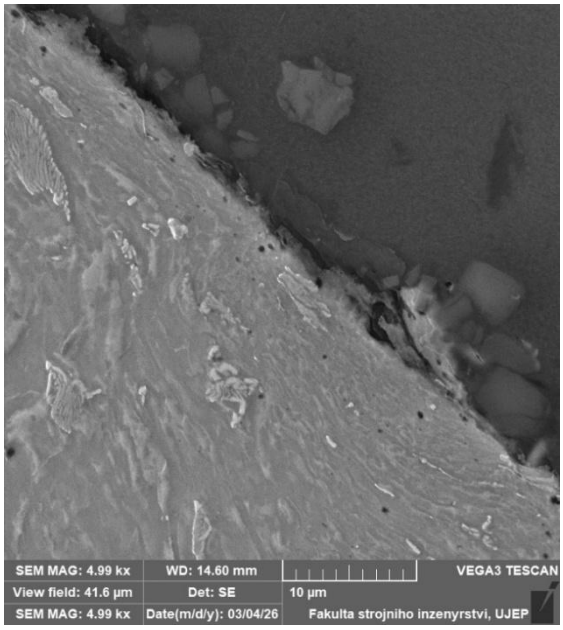

Fig. No. 25 – Detail from the interface between the steel stud and the tip stud – Al alloy.

Detailed EDS analysis showed that the Al alloy diffused into the body of the stud. As this detail documents, the structure of the stud is very deformed at the interface between the steel and the aluminum tip.

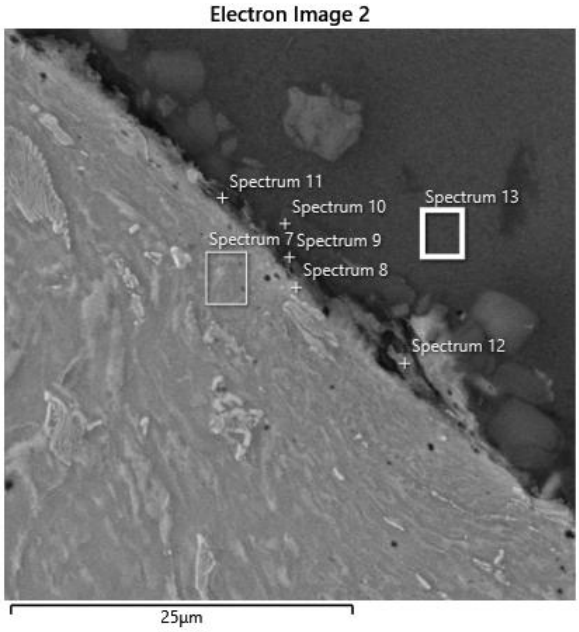

Fig. No. 26 – An EDS analysis was carried out in individual areas: spectrum 7 – 97,7 % Fe; 1,9 % Al; 0,4 % Mn; In all point EDS analyses at the steel - Al alloy interface, Al or Fe was detected and, depending on the amount of both elements, subsequently also Si or Mn.

Weld join– Stud No. 1

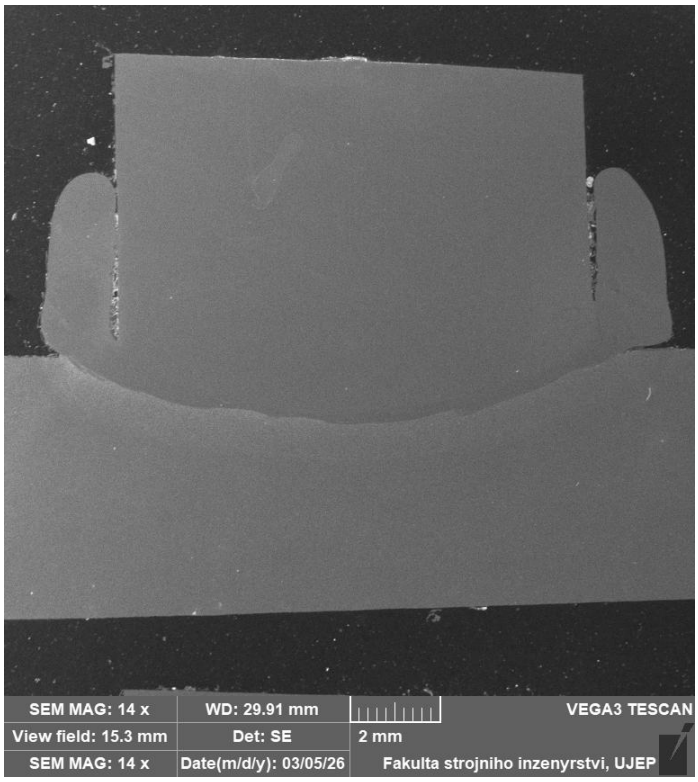

Fig. No. 27 – Joint – Stud 1 – mirror image of the metallographic microscope image

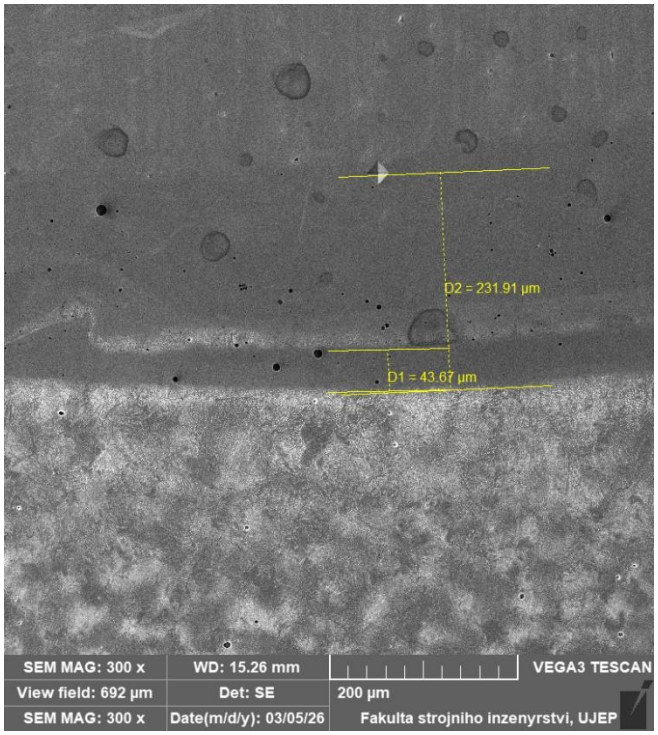

Fig. No. 28 – The middle part – captured indentation HV 0.1 – is at a distance of 0.23 mm from the interface.

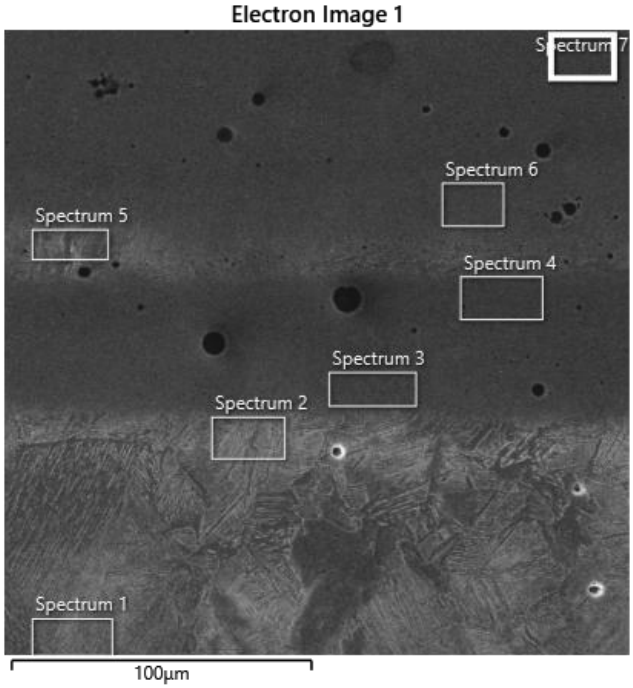

Fig. No. 29 – EDS analysis was performed - the middle part of the weld and it was found:
Spectrum 1 – 99,2 % Fe; 0,5 % Mn; 0,4 % Si;
Spectrum 2 – 98,8 % Fe; 0,5 % Mn; 0,4 % Cr; 0,3 % Si;
Spectrum 3 – 85,6 % Fe; 0,9 % Mn; 8,4 % Cr; 0,7 % Si; 4,4 % Ni;
Spectrum 4 – 84,0 % Fe; 0,9 % Mn; 9,1 % Cr; 0,8 % Si; 5,2 % Ni;
Spectrum 5 – 96,6 % Fe; 0,5 % Mn; 1,8 % Cr; 0, 4 % Si; 0,7 % Ni – again ordinary steel S355;
Spectrum 6 – 83,4 % Fe; 0,8 % Mn; 9,5 % Cr; 0,7 % Si; 5,4 % Ni;
Spectrum 7 – 79,1 % Fe; 1,1 % Mn; 12,3 % Cr; 0,8 % Si; 6,7 % Ni.

As documented by the content of individual elements, there were so-called strips of ordinary steel (welded plate made of S355 steel) at the weld interface in the stainless steel area (Stud). On the Stud side, the amount of chromium (nickel) in the interface area was reduced, below 12%Cr, i.e. this area is susceptible to possible corrosion.
In Stud 1, no significant carbides were detected on the stainless steel side along the austenitic grain boundary (basic structure of Stud, as it is austenitic steel Wr.N. 1.4541).

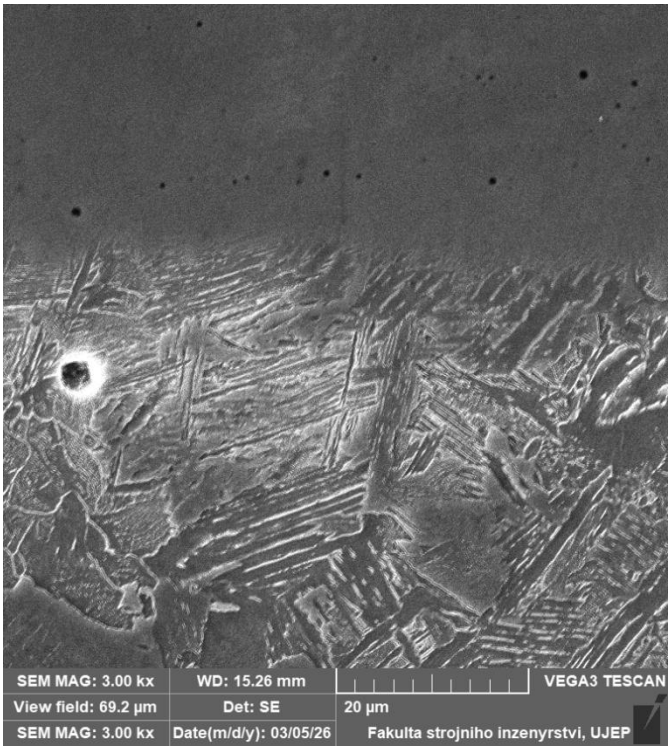

Fig. No. 30 – Middle part – detail of welded plate S355 – weld interface – cloudy structure of lower bainite. Martensite was present in this sample only in isolated cases.

As the following image from the edge of the Stud (right part) shows, in this area the underlying S355 material was not heated enough to create conditions for a cloudy structure of the lower bainite type.

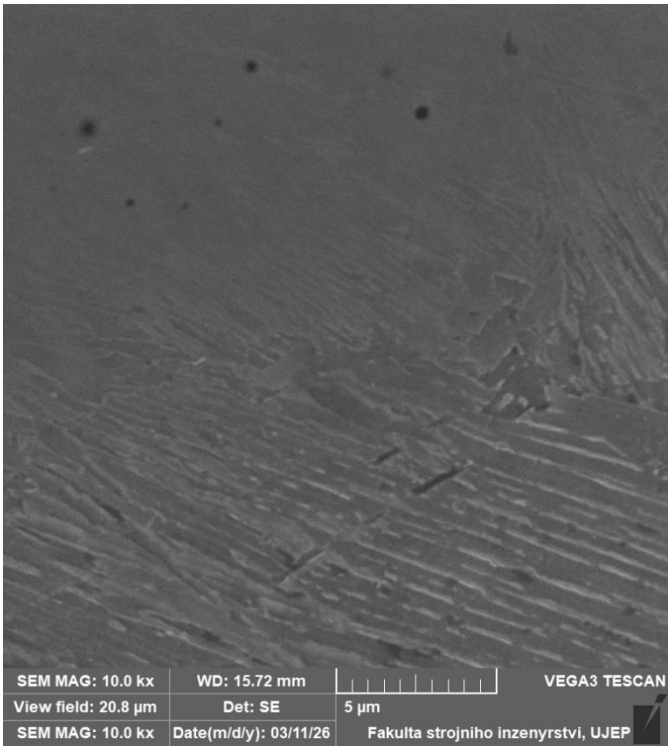

Fig. No. 31 – Right marginal part – interface on the S355 side – upper bainite occurs here, which further from the interface transitions into a pearlitic structure.

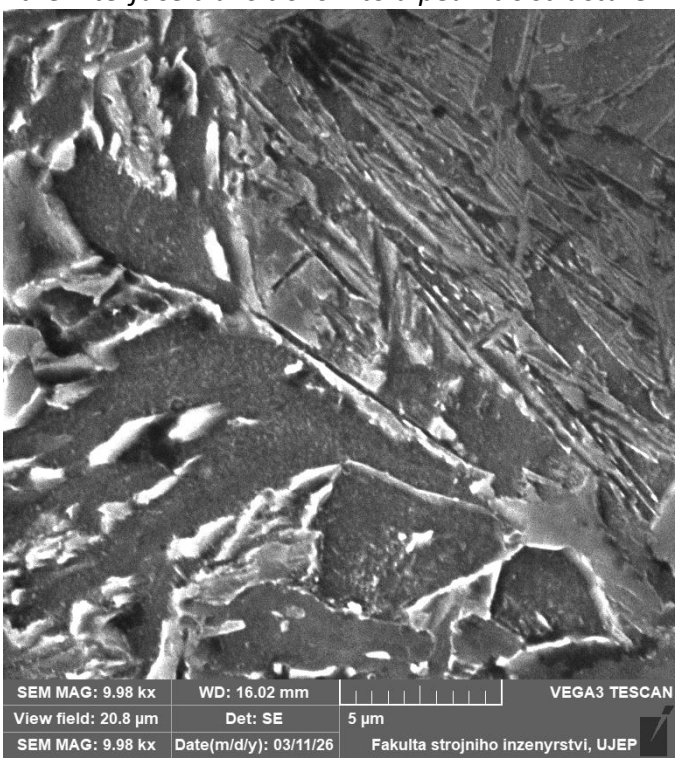

Fig. No. 32 – The left edge part – the interface on the S355 side – here there is a martensite region (the width of the martensite region is about 10 µm) and carbides are also present along the grain boundaries. As can be seen from Fig. No. 31 and 32, there is a relatively fundamental difference between the two regions (right – left), this difference is also between the center of the weld (in the Stud axis).

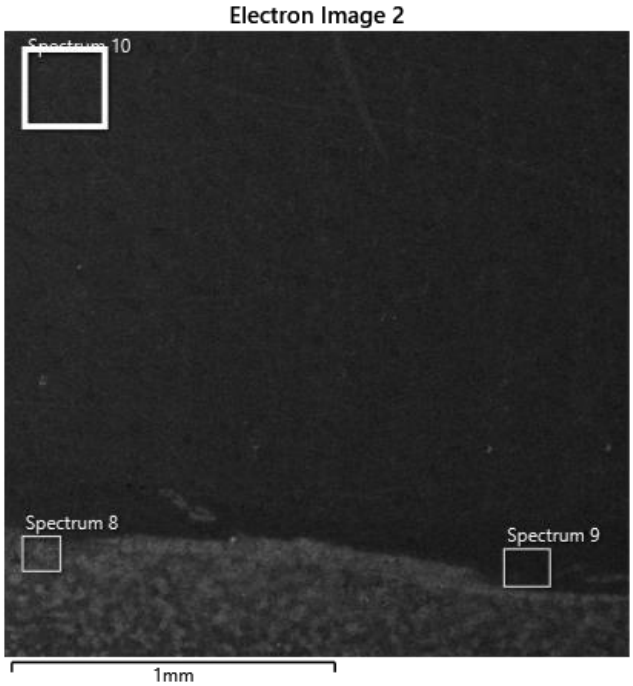

Fig. No. 33 – EDS analysis documents the difference between the interface and the more distant area of the Stud – it was found: Spectrum 8 – 98.7 % Fe; 0.5 % Mn; 0.5 % Si; 0.3 % Cr; Spectrum 9 – 83.7 % Fe; 1.1 % Mn; 8.8 % Cr; 0.9 % Si; 4.9 % Ni; 0.6 % Al – the presence of Al from the Stud tip was evident here; Spectrum 10 – 69.9 % Fe; 1.3 % Mn; 18.2 % Cr; 10.3 % Ni; 0.3 % Ti – Wr.N. 1.4541 steel contains Ti – carbide stabilization – TiC – prevention of carbide $Cr_{23}C_6$ formation.

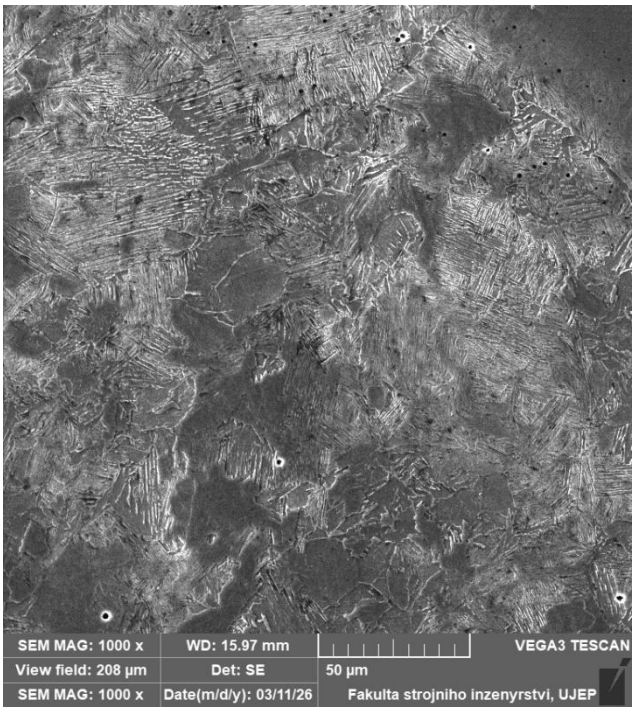

Fig. No. 34 – The left edge part – the S355 steel area – is at the top right is Stud Wr.N. 1.4541.

Weld join– Stud No. 2

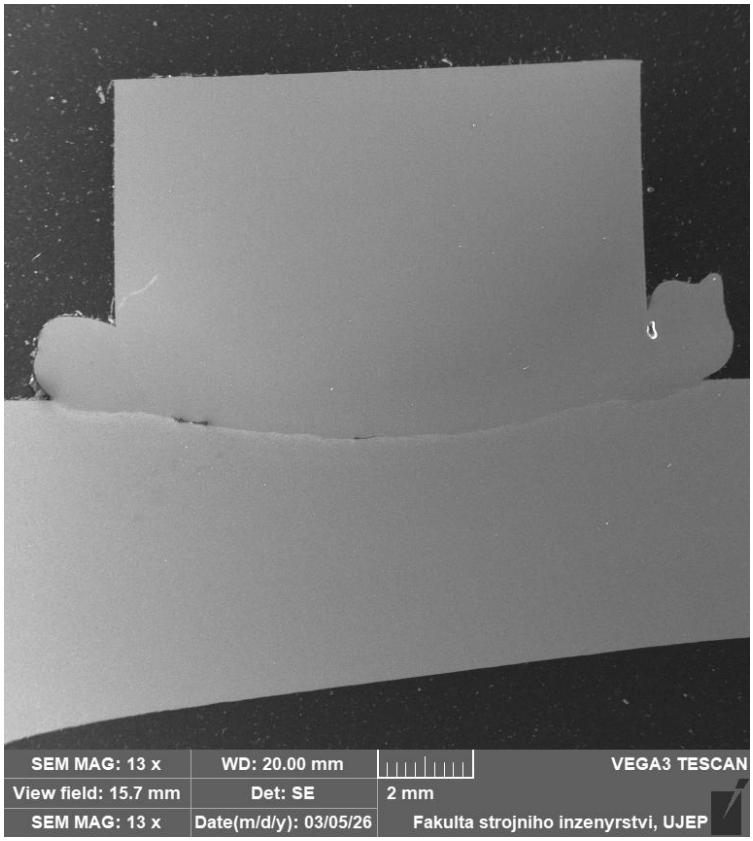

Fig. No. 35 – Joint – Stud 2 – mirror image of the metallographic microscope image

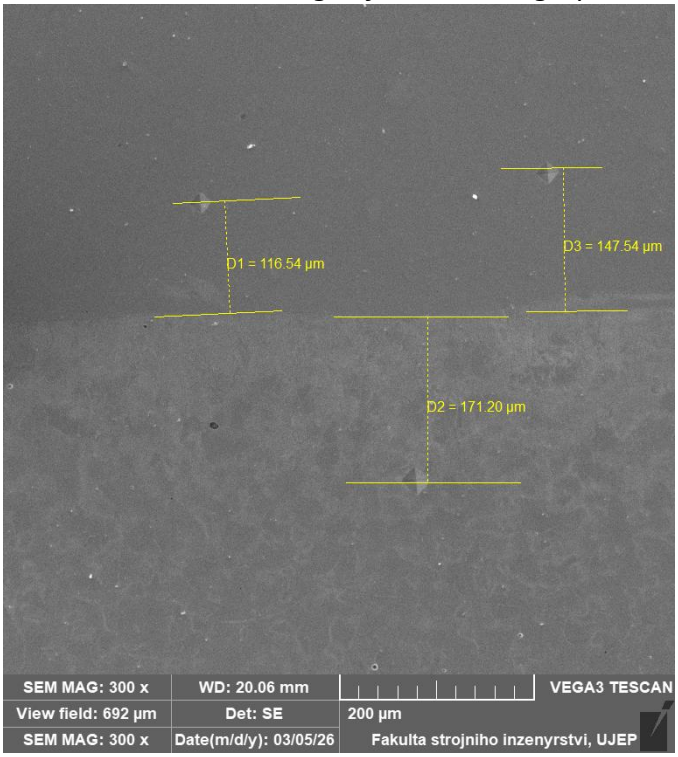

Fig. No. 36 – Distance of individual indentations HV0.1 in the middle part of the weld (middle part – longitudinal axis of the stud).

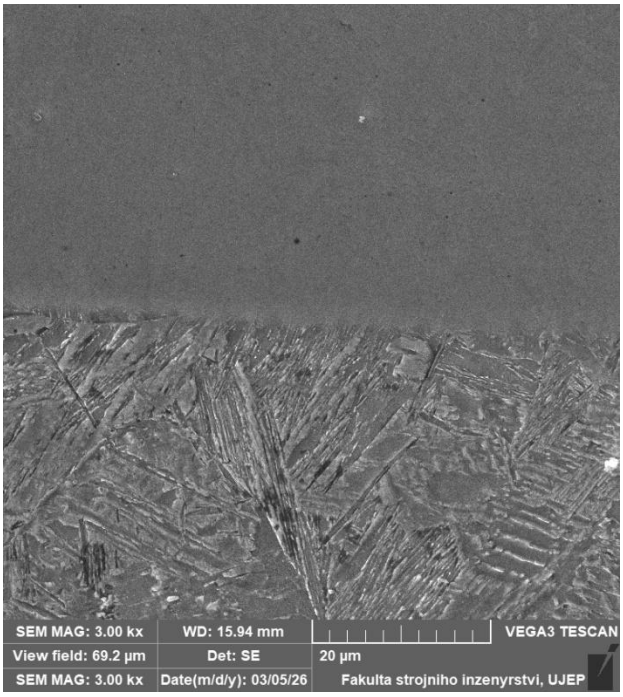

Fig. No. 37 – In the middle part in the interface area, lower and upper bainite occur, i.e. a cloudy structure. Along the boundaries of the original austenitic grains (on the S355 steel side) there are clear "chains" of carbides. Their chemical composition corresponds to the EDS results (Fe, Mn)$_3$C and also to chromium carbides (see spectrum 2).

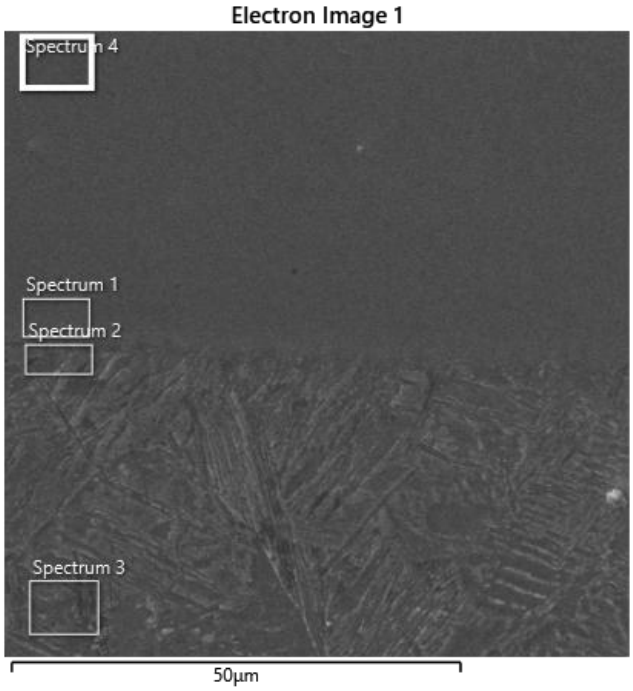

Fig. No. 38 – In the middle part (Fig. No. 16) EDS analysis was performed and it was found:
Spectrum 1 – 83.2 % Fe; 9.5 % Cr; 4.9 % Ni; 0.9 % Mn; 0.7 % Al; 0.6 % Si – in the interface area on the side of the steel Wr.N. 1.4541 there is also Al-Si – a residue from the tip of the Stud.
Spectrum 2 – 96.4 % Fe; 1.8 % Cr; 0.6 % Ni; 0.6 % Mn; 0.5 % Si;
Spectrum 3 – 99.2 % Fe; 0.5 % Mn; 0.3 % Cr;
Spectrum 4 – 73 % Fe; 15.4 % Cr; 8.3 % Ni; 1.3 % Mn; 1.2 % Al; 0.8 % Si.

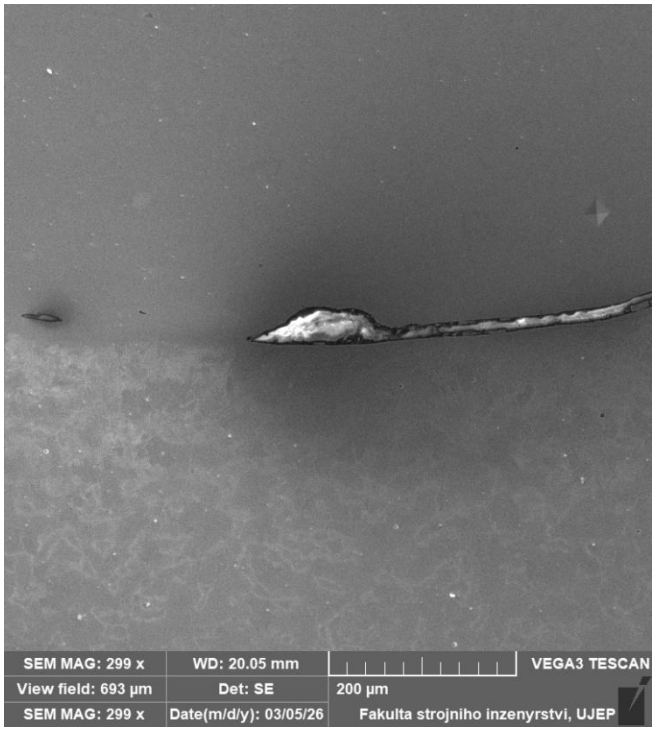

Fig. No. 39 – Defect at the interface of the weld joint – the defect is near the middle (axial part of the weld)).

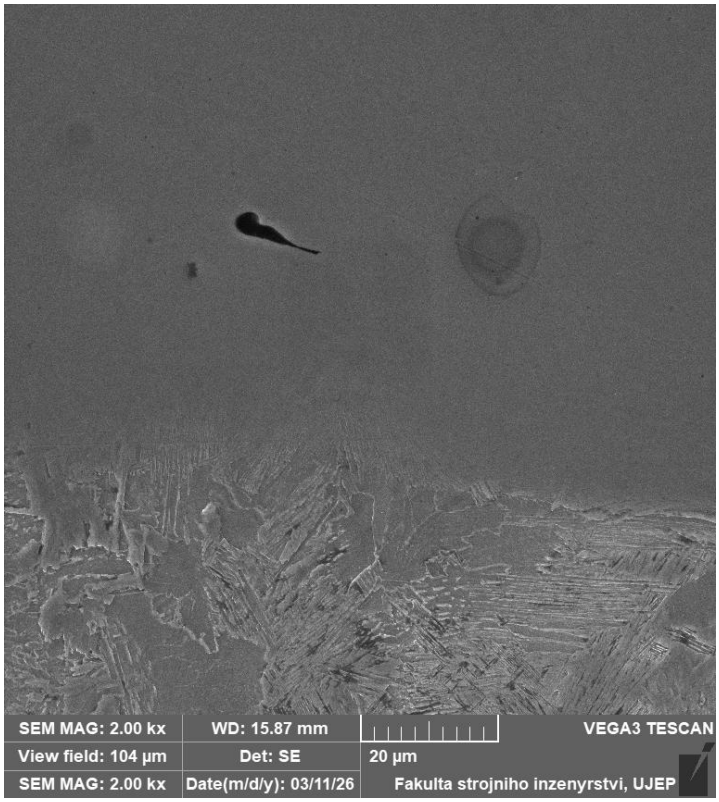

Fig. No. 40 – Due to high metallurgical pressures during cooling, the original pore was deformed.

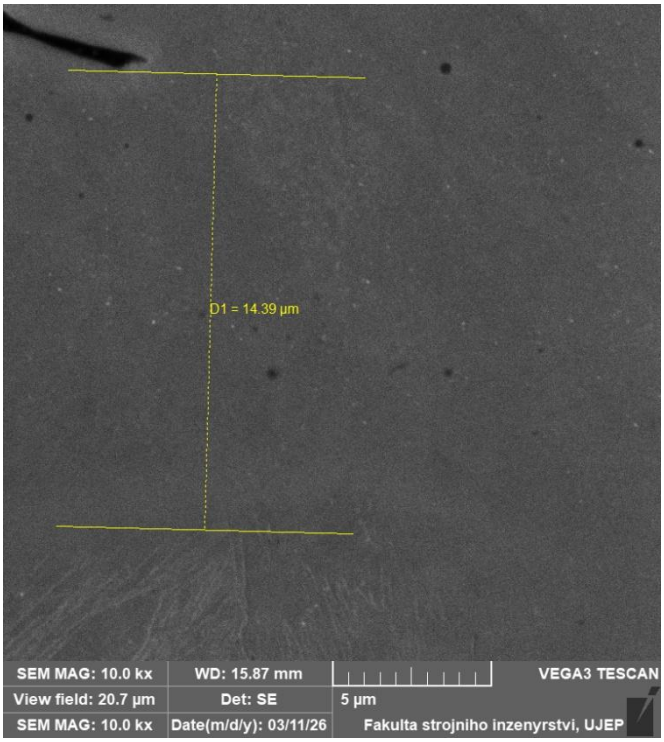

Fig. No. 41 – The defect is not exactly at the interface, but is about 14 µm from the interface.

Due to the lower thermal conductivity of Wr.N. 1.4541 steel, S355 steel melts more, therefore the weld metal is mixed more with steel without chromium and nickel, but on the other hand with a higher carbon concentration (approx. 0.23%C).

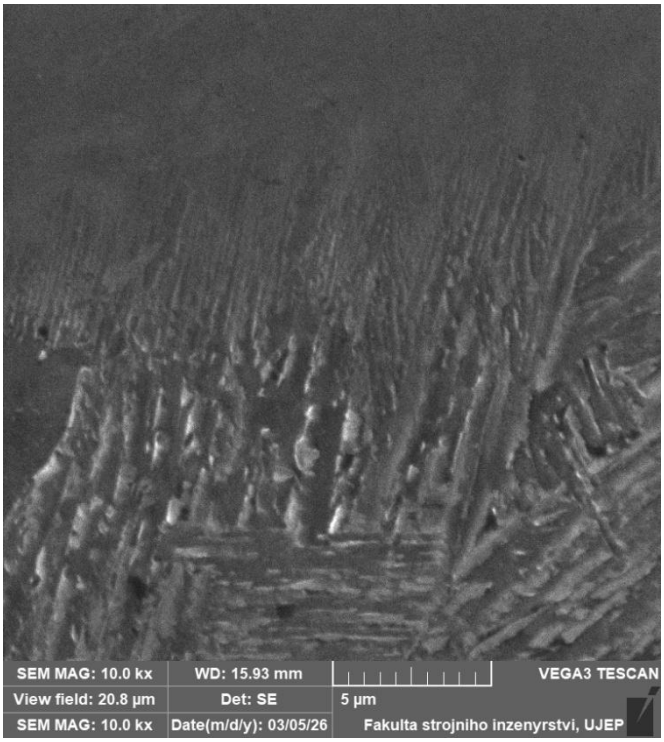

Fig. No. 42 – Interface – structural condition on the S355 steel side – weld edge Studs – carbides (Fe_3C, but also $Cr_{23}C_6$) are directed by heat removal – upper bainite.

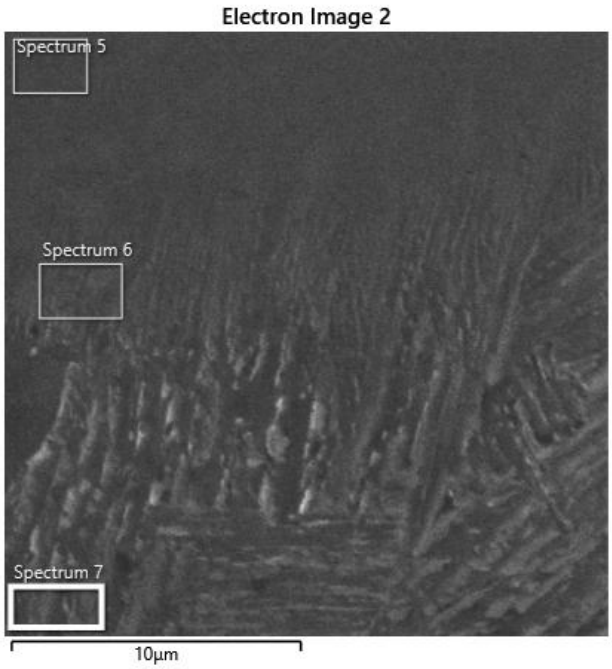

Fig. No. 43 – EDS analysis was performed in the marked areas:
Spectrum 5 – 83,4 % Fe; 9,4 % Cr; 5,0 % Ni; 0,9 % Mn; 0,7 % Si; 0,6 % Al; Spectrum 6 – 92,4 % Fe; 4,2 % Cr; 2,2 % Ni; 0,7 % Mn; 0,5 % Si; Spectrum 7 – 98,0 % Fe; 1,0 % Cr; 0,6 % Mn; 0,5 % Si.

Weld join– Stud No. 3

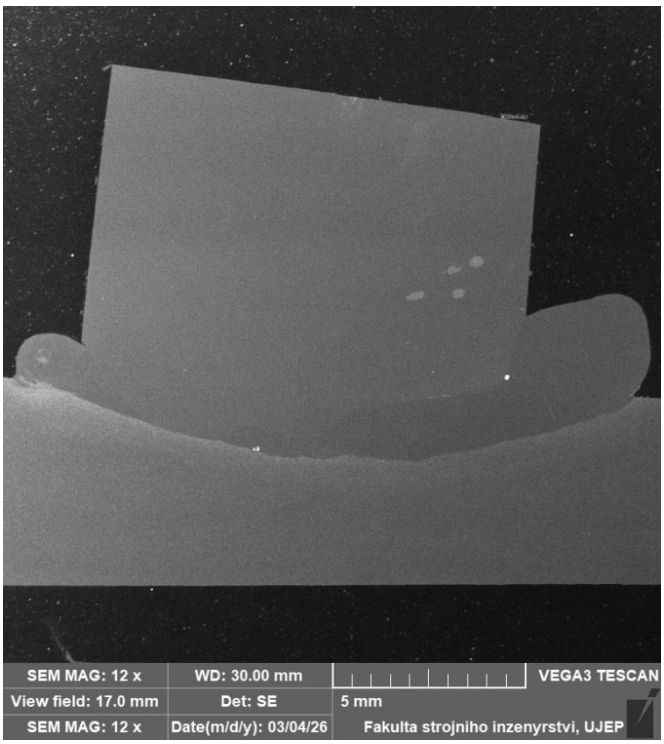

Fig. No. 44 – Joint – Stud 3 – mirror image of the metallographic microscope image.
This Stud was not welded straight, as evidenced by the different size of the spall material. This also resulted in uneven weld metal and thus different chemical composition in individual areas of the Stud – this is better seen on the light microscope. See Fig. 44A (below)

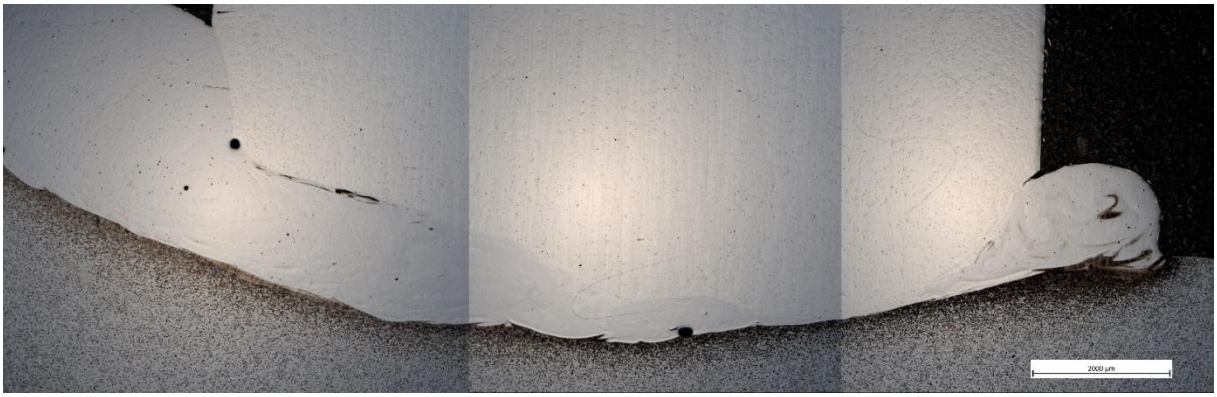

Fig. No. 44A (auxiliary image) – join – Stud 3

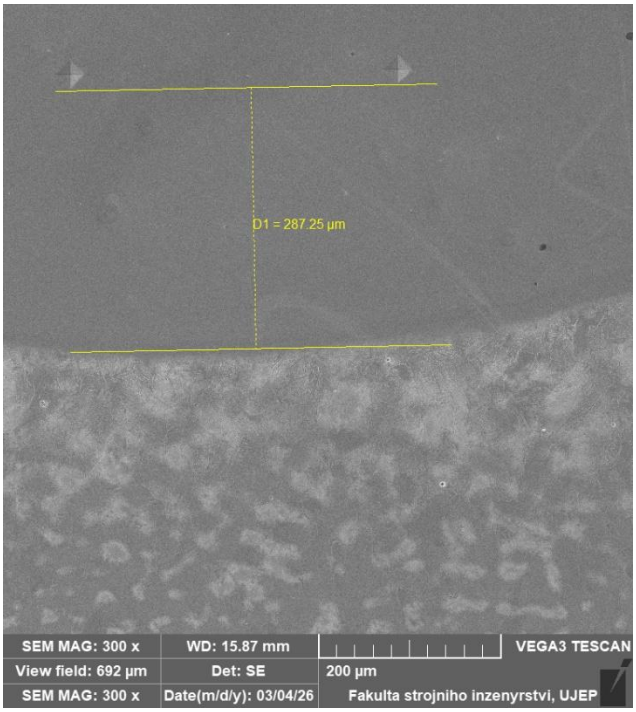

Fig. No. 45 – Distance of indentations from the fusion interface – middle part of the samples

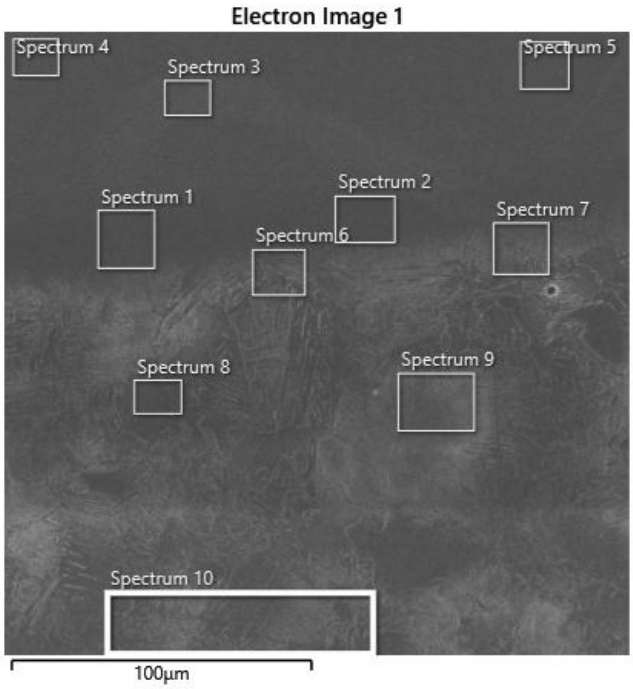

Fig. No. 46 – Picture of individual spectra in the middle part of the Stud weld.
In spectrum 1 at the interface, it was found: 11.5 % Cr; 6.2 % Ni; 1.0 % Mn; 0.8 % Si; 0.7 % Al – comes from the Stud tip. Spectrum 2 had a similar chemical composition, spectrum 3 already contained more Cr and Ni – 16.7 % Cr; 9.1 % Ni; 1.2 % Mn; 1.0 % Si; 0.8 % Al; 0.2 % Ti – titanium is used to stabilize carbides and prevent the formation of chromium carbides. Other spectra 4 and 5 had the same chemical composition as spectrum 3. Spectrum 6, i.e. already on the S355 steel side, had the following chemical composition: 1.4 % Cr; 0.6 % Ni; 0.5 % Mn; 0.3 % Si (the same result was in spectrum 7); spectrum 8; 9 and 10 were already completely free of Cr and Ni and had around 0.5 % Mn and 0.4 % Si.

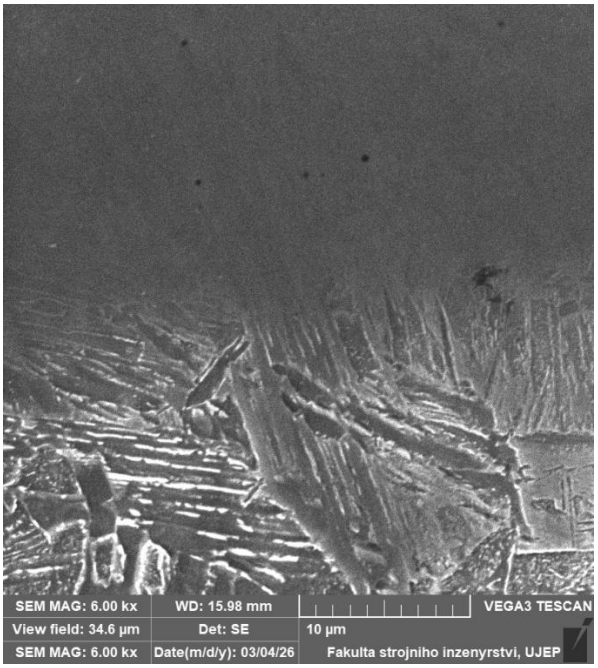

Fig. No. 47 – Detail of the interface – upper bainite occurs in this area – the most prominent structure, in some areas lower bainite is captured transforming into martensite (completely at the interface).

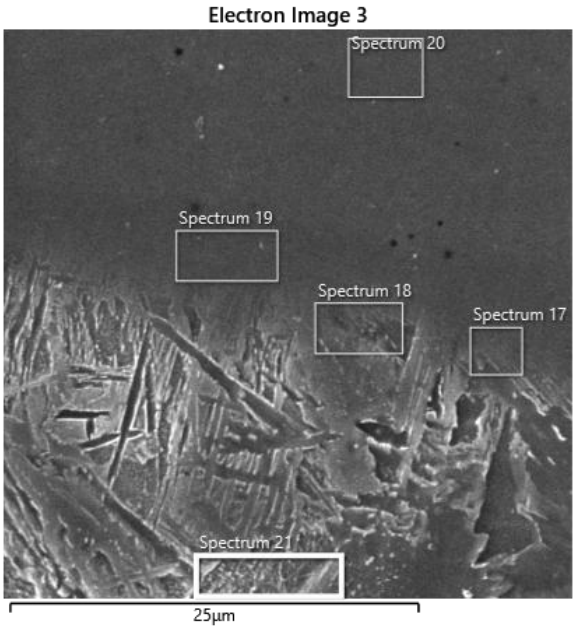

Fig. No. 48 – Picture of individual spectra in the middle part of the Stud weld.
In spectrum 17 at the interface towards S355 it was found: 5.0 % Cr; 2.5 % Ni; 0.7 % Mn; 0.6 % Si (spectrum 18 also shows the presence of Cr – around 3.3 %);
spectrum 19 - 10.8 % Cr; 5.8 % Ni; 1.0 % Mn; 0.7 % Si,
spectrum 20 contains 15.6 % Cr; 8.5 % Ni; 1.1 % Mn; 0.8 % Si; 1.0 % Al.
Spectrum 21 also contains 0.3 % Cr, which demonstrates the diffusion of chromium to a relatively large distance.

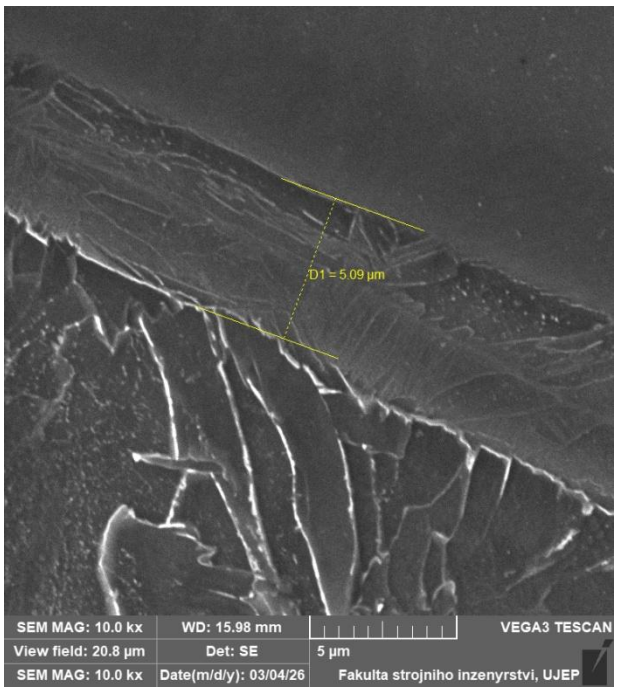

Fig. No. 49 – Left part of the weld (according to SEM image – Fig. No. 44).
There is not a large area of weld metal in this area, i.e. the stud here does not have extensive TOO and its original concentration (18 %Cr and 10%Ni) goes up to the weld with steel S355. In this area there are extensive carbides along the grain boundaries and in this area the risk of intergranular corrosion can be expected.

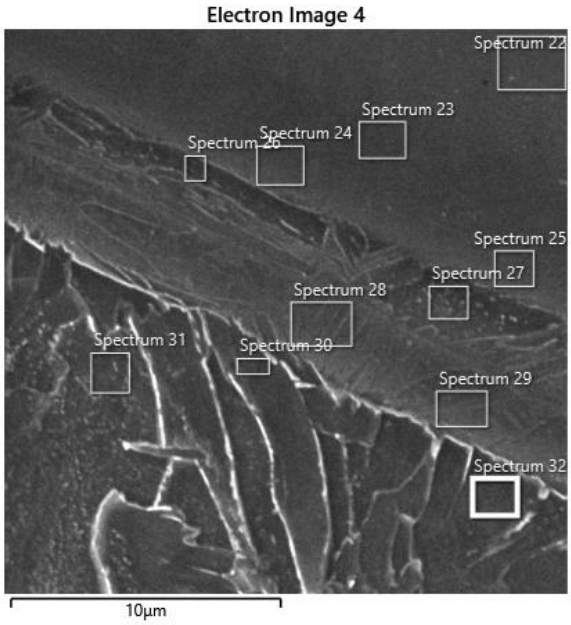

Fig. No. 50 – Pictures of individual spectra in the left part of the Stud weld.
In spectrum 22 (Stud): 16.5 % Cr; 9.3 % Ni; 1.0 % Mn; 1.0 % Si; 0.7 % Al.
In spectra 23; 24; 25, the concentration of chromium and nickel was already decreasing, however, this decrease was slower than in the middle part of the Stud, or in the part where there was a large area of weld metal. At the interface – spectrum 26 – at the interface between the Stud and the building area – a 5 µm wide strip contains 4.7 % Cr and 2.1 % Ni. This entire strip has a concentration in the range of 4 to 5 % Cr and the corresponding Ni. The concentration of chromium on the S355 steel side is decisive – spectrum 30 to 32 – here the chromium concentration was around 1.2 % Cr.

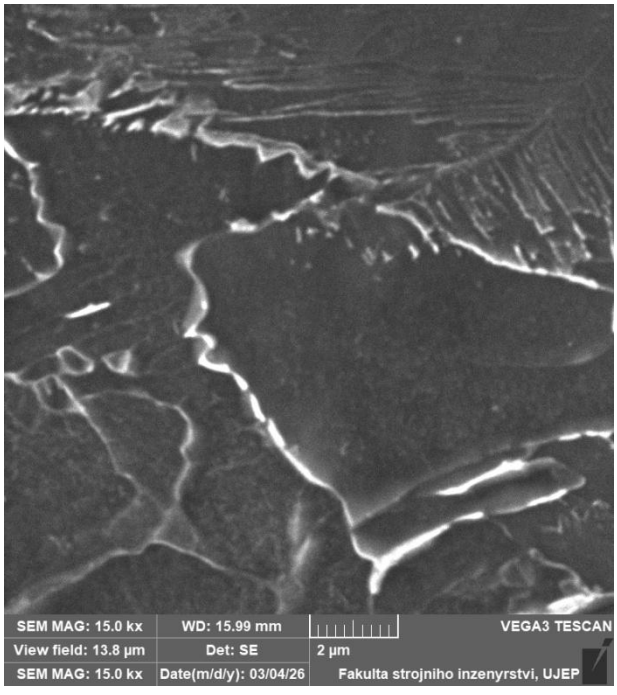

Fig. No. 51 – Detail of carbides along the original austenitic grain boundary.
These carbides contain a medium amount of chromium, but they are not the classic $Cr_{23}C_6$ carbides, but rather Fe_3C carbides, which also contain chromium (around 1%Cr).

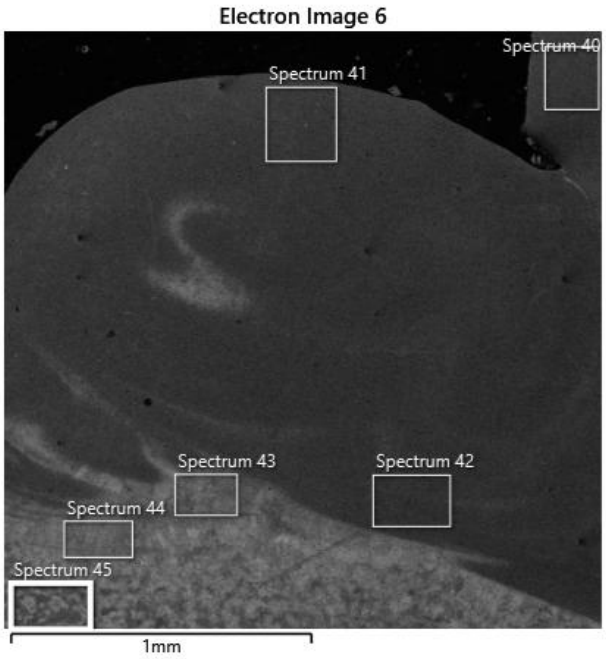

Fig. No. 52 – The left part of the slag captures the weld metal - the records of individual spectra document its chemical composition: spectrum 40 (Stud): 18.5 % Cr; 10.2 % Ni; 1.5 % Mn; 0.7 % Si. Spectrum 41: 10.5 % Cr; 5.1 % Ni; 0.9 % Mn; 1.3 % Si. Spectrum 42: 7.0 % Cr; 3.3 % Ni; 0.9 % Mn; 0.9 % Si. Spectrum 43 (already S355 steel – surface): 1.6 % Cr; 0.9 % Ni; 0.7 % Mn; 1.0 % Si. Spectrum 44: 1.4 % Cr; 0.4 % Ni; 0.7 % Mn; 0.9 % Si. Spectrum 45: 0.2 % Cr; 0.5 % Mn.

Weld join– Stud No. 4

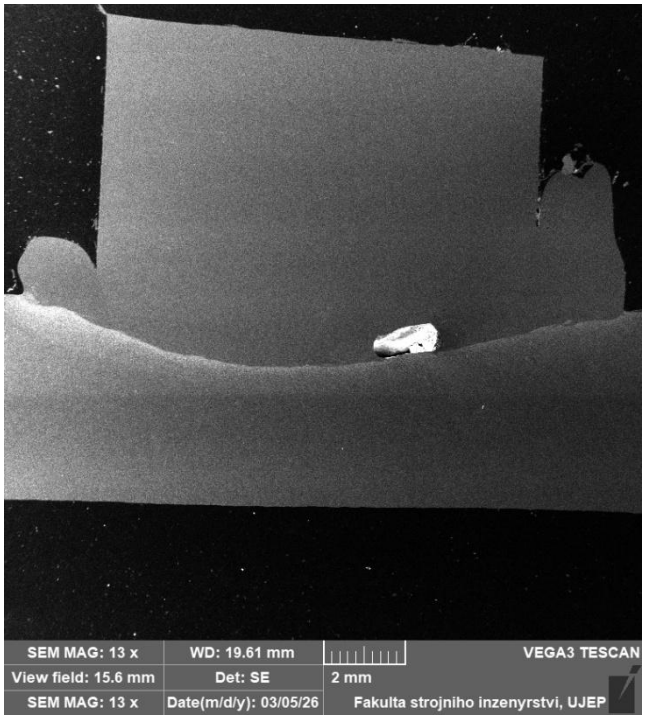

Fig. No. 53 – Joint – Stud 4 – mirror image of the image from the metallographic microscope. This stud also has an irregular protrusion, and a defect – a pore – is also discernible, which upon closer examination has the character of a dropped inclusion (Fig. No. 54).

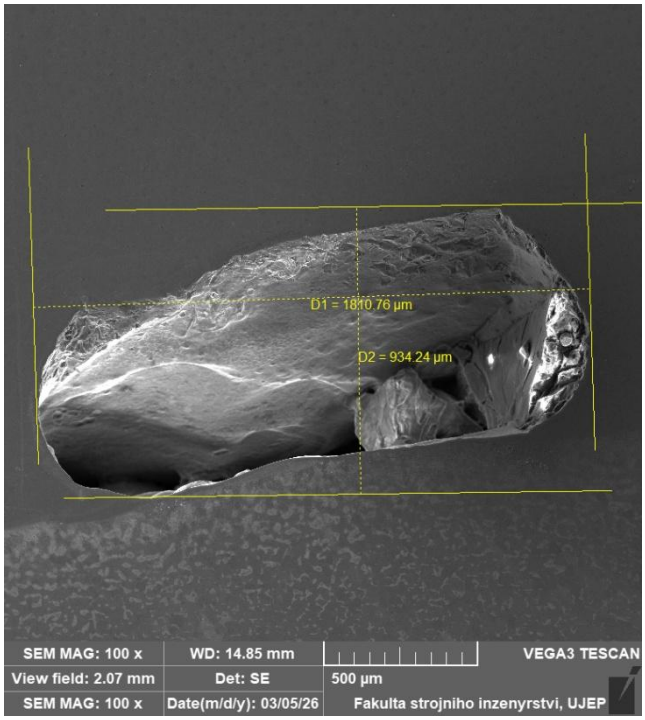

Fig. No. 54 – Detail of the defect at the interface of the weld and the S355 steel – building side

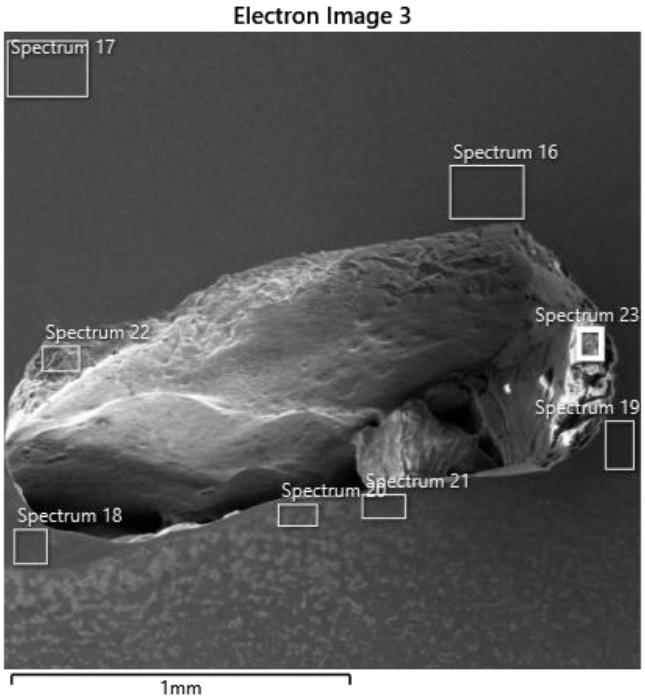

Fig. No. 55 – Pictures of individual spectra at the defect site.
In spectrum 16 and 17 (Stud) the classical chemical composition corresponds to Wr.N. 1.4541.
Spectrum 18: 8.8 % Cr; 4.6 % Ni; 0.9 % Mn; 0.9 % Si.
Spectrum 19: 13.9 % Cr; 7.5 % Ni; 1.0 % Mn; 0.9 % Si; 0.6 % Al.
Spectrum 20; 21 – chemical composition corresponding to S355 with the presence of chromium up to 0.5 % Cr.
Spectrum 22; 23 was directly from the defect site and contains – spectrum 22: 12.3 % Cr; 3.6 % Ni (chromium segregation); 22.2 % Al; spectrum 23: 61.0 % Al; 10.7 % Si; 7.7 % Cr; 7.4 % Fe; 4.7 % Mn; 3.9 % Mg; 3.6 % Ti; 1.0 % Ca – aluminum-based oxide inclusion (corundum).

Further details were photographed and EDS analyses were performed at the defect site, confirming that it was an Al-based oxide inclusion.

Another interesting feature is Fig. No. 56 documenting an oxide inclusion in a location that was not considered weld metal, i.e. it was assumed that this area falls into the TOO category.

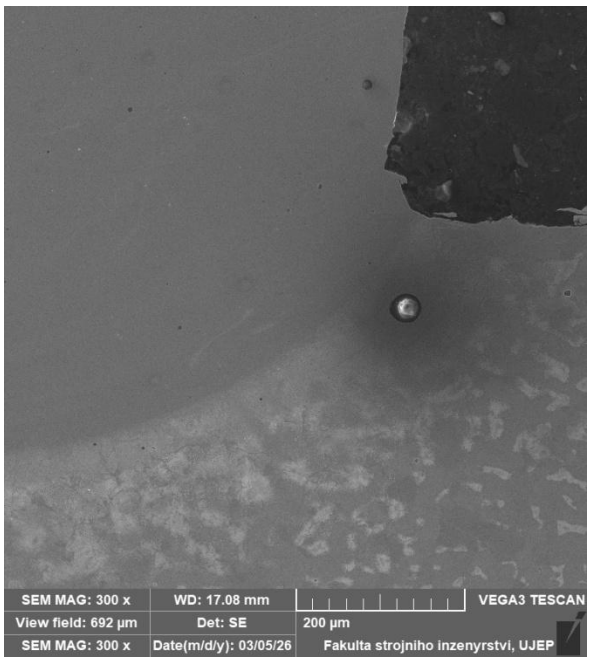

Fig. No. 56 – Detail of a defect whose location in the TOO is unjustifiable.

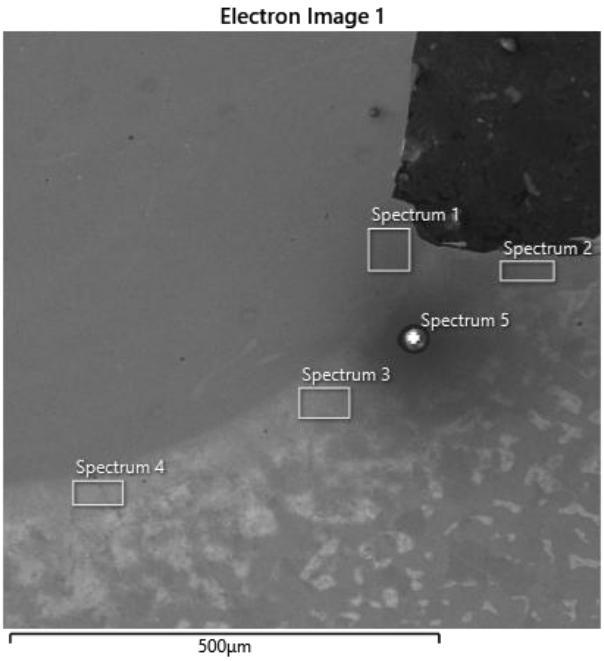

Fig. No. 57 – Picturess of individual spectra at the defect location.
Spectrum 1: 11.2 % Cr; 6.4 % Ni; 1.2 % Si; 1.0 % Mn; 0.5 % Al.
Spectrum 2 – 0.4 % Si; 0.4 % Mn, the rest Fe – chromium was intentionally measured here and the result was zero concentration.

Spectrum 3 – 1.4 % Cr; 0.9 % Mn; 0.7 % Si; 0.7 % Ni – this means this is an area of S355 steel – this spectrum is at the same distance from the building boundary as the monitored defect. Spectrum 4 – 1.5 % Cr; 0.9 % Si; 0.7 % Mn; 0.6 % Ni – an area that is closer to the building boundary, and yet it is a TOO at the S355 location. Spectrum 5 (defect): 50.6 % O; 23.9 % Al; 13.9 % Si; 4.0 % Fe; 2.6 % Mg; 2.0 % Mn; 1.6 % Cr; 0.5 % Ti; 0.5 % K; 0.3 % Ca.

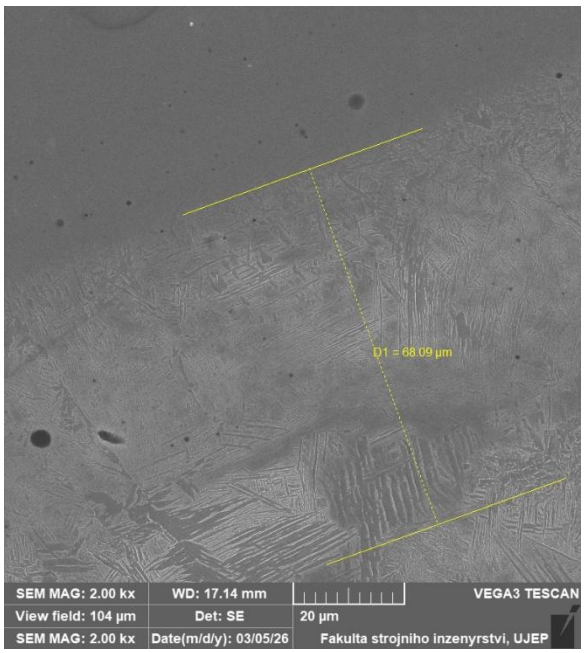

Fig. No. 58 – Based on the previous result, it is estimated that an area of approximately 70 µm in the S355 steel was also melted, i.e. it is not TOO, but weld metal.

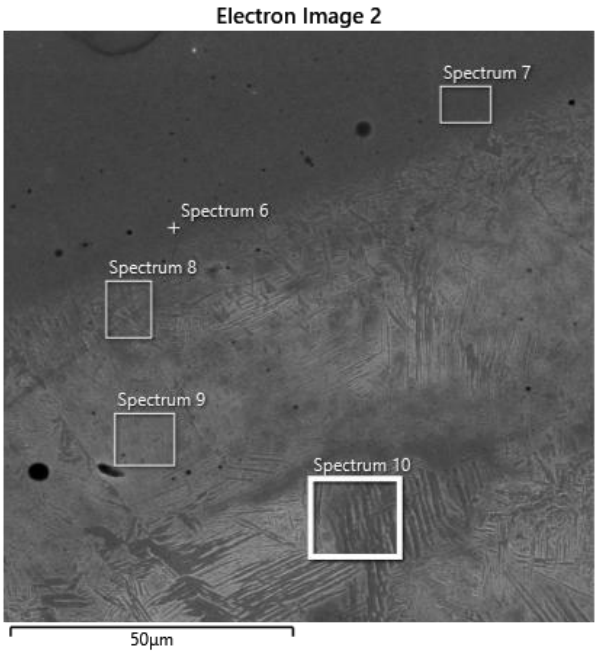

Fig. No. 59 – In the area where melting occurred (according to the monitored pore), EDS analysis was performed: Spectrum 6 -7.1 % Cr; 3.3 % Ni; 0.8 % Si; 0.7 % Mn; Spectrum 7 - 7.1 % Cr; 3.6 % Ni; 1.1 % Si; 0.9 % Mn; Spectrum 8 – 1.9 % Cr; 0.7 % Mn; 0.7 % Si; 0.6 % Ni; Spectrum 9 – 1.5 % Cr; 0.8 % Mn; 0.7 % Si; 0.56 % Ni; Spectrum 10 – 0.6 % Mn; 0.3 % Si – this area is no longer chromium-free.

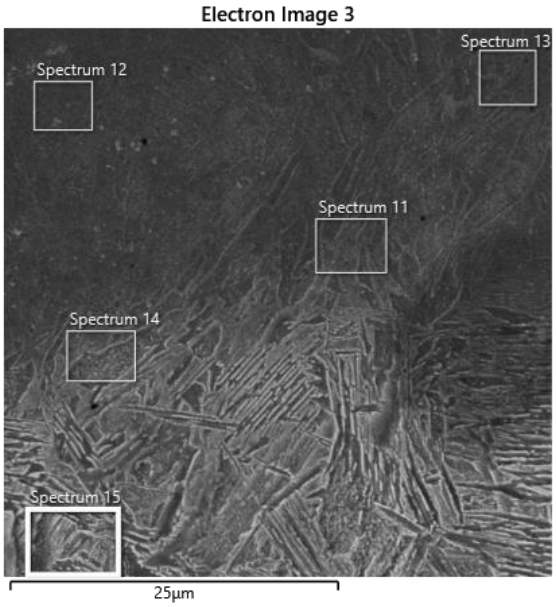

Fig. No. 60 – Different area than the previous image, but still the building interface. Spectrum 11 -3.9 % Cr; 2.2 % Ni; 0.8 % Mn; Spectrum 12 – 5.2 % Cr; 2.7 % Ni; 0.6 % Si; 0.9 % Mn; Spectrum 13 – 4.4 % Cr; 1.0 % Mn; 2.6 % Ni; Spectrum 14 – 2.8 % Cr; 0.7 % Mn; 0.7 % Si; 1.3 % Ni; Spectrum 15 – 0.6 % Mn; 0.6 % Cr.

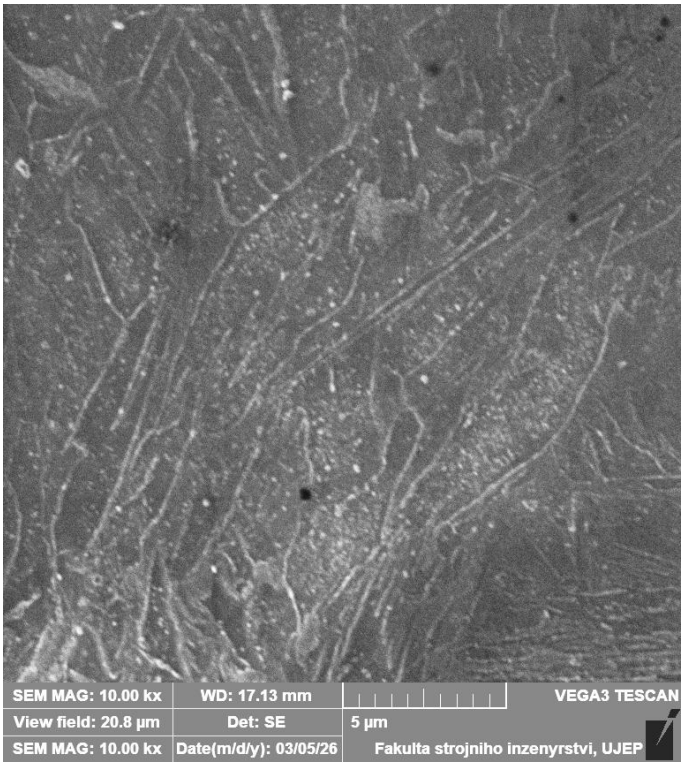

Fig. No. 61 – Only at the Stud 4 joint were these small but continuous carbides detected along the austenitic grain boundaries at the Stud location, i.e. on the Wr.N. 1.4541 steel side. Unfortunately, their size does not allow for their separate EDS analysis, but as in the previous case, they will probably be cementite-based carbides. However, their danger may be not only intergranular corrosion, but also embrittlement of the otherwise tough austenite.

ČVUT v Praze, Fakulta strojní, Ústav strojírenské technologie, Technická 4, Praha 6, 166 07, Česká republika
T 224 352 628 E 12133@fs.cvut.cz W u12133.fs.cvut.cz

Weld join– Stud No. 5

Fig. No. 62 – Joint – Stud 5 – overall scanning electron microscope image missing

Fig. No. 63 – Light microscope image – this location was also documented using a scanning electron microscope.

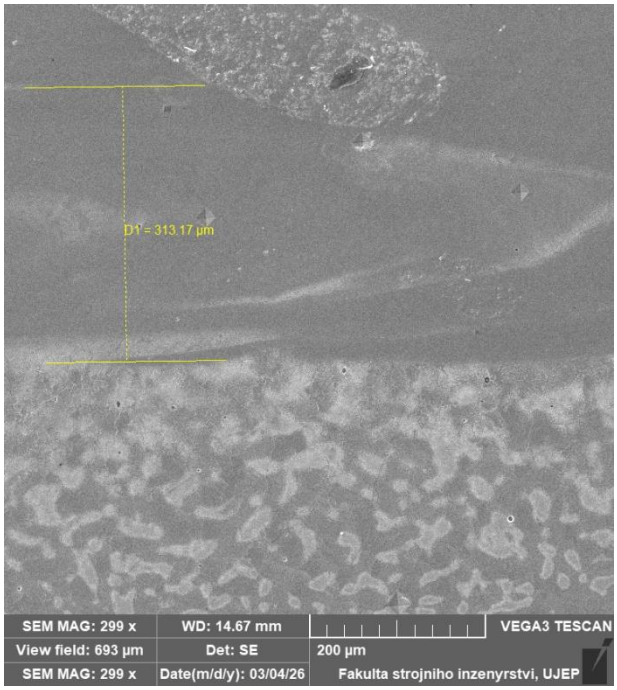

Fig. No. 64 – SEM image – showing impressions and the way the melt is mixed in the weld metal.

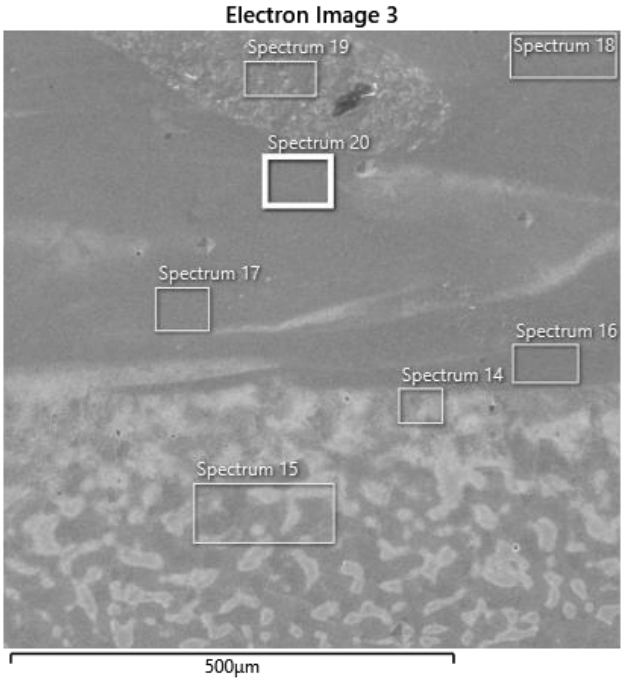

Fig. No. 65 – Middle area of the Stud joint, EDS analysis was performed in this area. As in previous cases, EDS analysis was performed on both sides of the construction boundary and the change in chromium concentration in the TOO and in the weld metal was monitored, and in the case of steel S355, the diffusing amount of chromium was monitored.

Spectrum 14 - 0.5 % Cr; 0.5 % Si; 0.4 % Mn; Spectrum 15 – 0.6 % Si; 0.5 % Mn;
Spectrum 16 – 10.4 % Cr; 0.9 % Mn; 0.6 % Si; 5.6 % Ni; 0.6 % Al.
Spectrum 17 – 6.8 % Cr; 0.9 % Mn; 0.7 % Si; 3.6 % Ni;
Spectrum 18 – 16.4 % Cr; 8.7 % Ni; 1.4 % Mn; 0.8 % Si;
Spectrum 19 – 11.2 % Cr; 6.0 % Ni; 1.2 % Mn; 1.0 % Si; 0.9 % Al;
Spectrum 20 – 10.6 % Cr; 5.8 % Ni; 1.1 % Mn; 0.6 % Si; 0.7 % Al.

As documented by the chemical composition, aluminum (alloy) is present in the weld metal, which probably comes from the tip of the Stud.

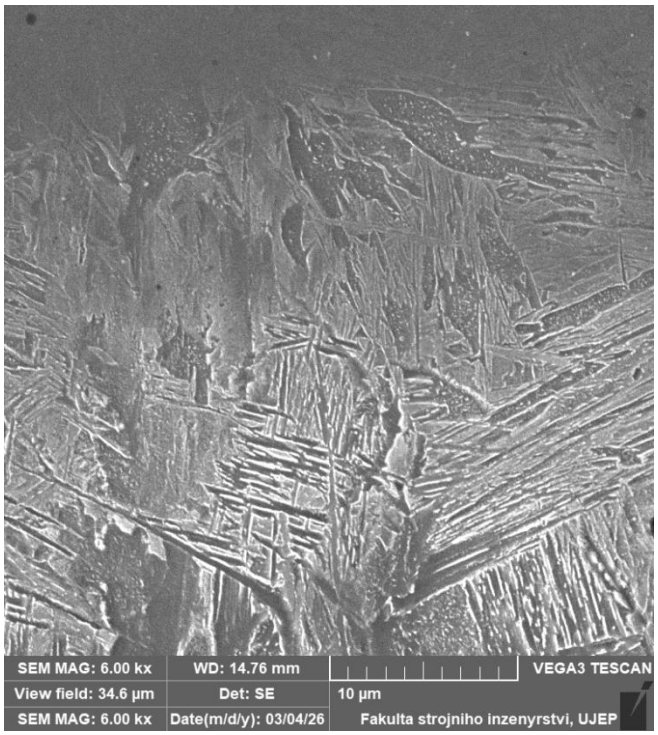

Fig. No. 66 – Detail of the underlying steel S355 at the boundary of the building – the structure is formed by lower bainite, which transitions into upper bainite. No significant carbides were detected at the boundary.

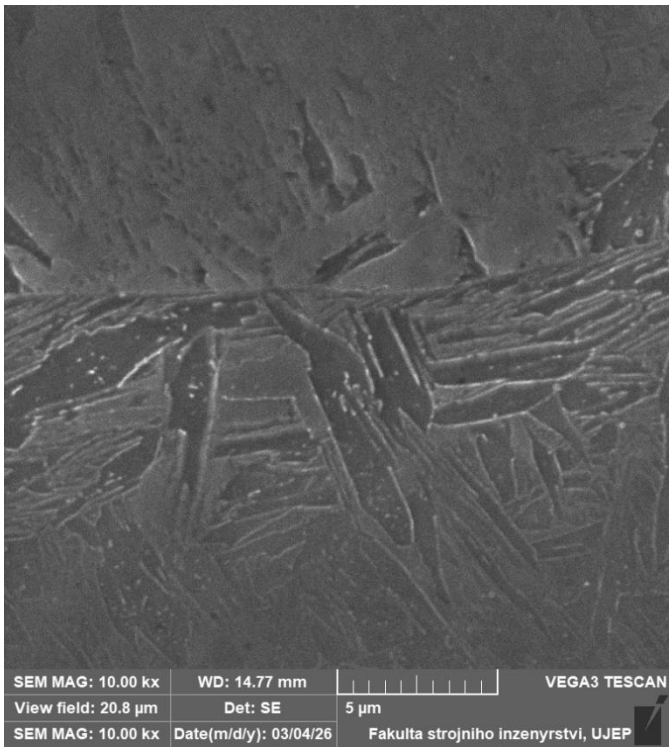

Fig. No. 67 – This image documents the interface area between the Stud area and the underlying S355 steel. The extent of the mixing is documented by the EDS analysis results.

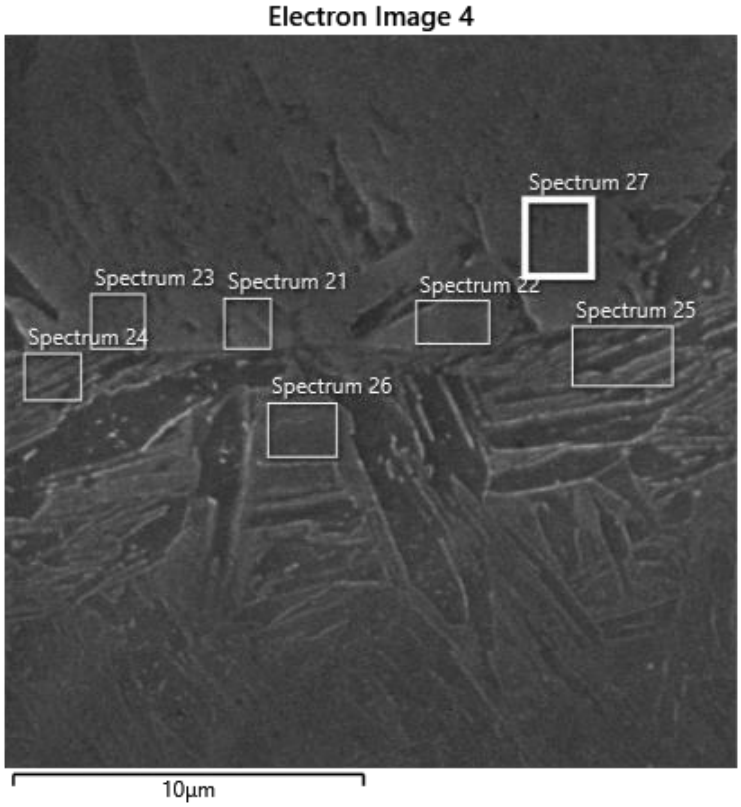

Fig. No. 68 – Results of EDS analysis in the middle part of the Stud.
Spectrum 21 – 3.0 % Cr; 1.5 % Ni; 0.5 % Si; 0.6 % Mn;
Spectrum 22 – 2.7 % Cr; 1.5 % Ni; 0.5 % Si; 0.6 % Mn (similar area to Spectrum 21) and also similar chemical composition, which showed a change in chromium on the Stud side – in this area the weld metal is mixed with structural steel S355.
The same chemical composition was also in Spectrum 23.
Spectrum 24 (from the building towards S355) – 3.0 % Cr; 1.4 % Ni; 0.5 % Si; 0.7 % Mn.
Spectrum 25 – 3.0 % Cr; 1.1 % Ni; 0.5 % Si; 0.7 % Mn – in the area of S355 steel there is a relatively large amount of chromium, which is subsequently reflected in the structure (turbid structure) and the resulting microhardness values.
Spectrum 26 – 2.8 % Cr; 1.6 % Ni; 0.6 % Si; 0.7 % Mn;
Spectrum 27 – 3.4 % Cr; 1.7 % Ni; 0.6 % Si; 0.8 % Mn.

From the above chemical composition it follows that the concentration of chromium on the S355 steel side is relatively significant, and this affected the structural condition.

Conclusion

The final condition was most affected by the seating of the Stud made of Wr.N. 1.4541 steel on the S355 steel plate. In the case of uneven welding, the weld metal was pushed out to one side. In this case, not only the uneven build-up (spurt) was observed, but also the uneven area of the weld metal and the variable chemical composition of the weld metal. On the Stud side, the alloying elements (Cr, Ni) decreased to half and in some cases even to a third of the concentration.

Stud 1 (welding parameters: 850 A; 390 ms) – i.e. little heat, long time.
The stud is welded relatively evenly, both spatters are similar (i.e. on both sides of the cut). The weld metal has two layers, one is made of stainless steel with a reduced concentration of chromium and nickel (about 8 % Cr and 4 % Ni) and the second layer is made of structural steel S355 with the presence of chromium (about 2 % Cr). Lower bainite occurs below the build-up area at the interface with steel S355. Carbides are concentrated in larger formations and are also on the grain boundaries of steel S355. Carbides are not in the interface area. The structure showed a relatively long heating time – carbides clustered at the grain boundaries (in steel S355), they are larger. The hazy structure (bainitic) is so small that it was not affected by the microhardness measurement. From the point of view of the possible risk of corrosion, the structural condition of the two interpenetrating layers, the weld metal with a reduced concentration of Cr and Ni and the strip of structural steel S355 with increased chromium above this area is not good. No cloudy structure has formed here, because the heat dissipation into the austenite is limited by its low thermal conductivity. No chromium carbides are trapped, both on the weld metal side, in the TOO steel Wr.N. 1.4541, and on the plate of steel S355.

Stud 2 (1600A; 75 ms) – this Stud had a significantly larger amount of heat input, albeit for a short time, but rapid melting occurred.
The Stud is not completely perpendicular to the S355 steel plate, but the spalls have a similar shape. In the weld in the building area, a cold joint area is captured and pores are also captured that are deformed by the pressures of advancing crystallization. The structure in the weld metal is uniform and again with a reduced concentration of chromium and nickel. No chromium-based carbides were observed. On the side of the S355 structural steel, there is a larger area of opaque structure (bainite and in places martensite), which is also reflected in the course of microhardness. The corrosion risk aspect is smaller in this joint than in Stud 1 (heterogeneity in the weld metal), but in terms of brittle damage, Stud 2 is more susceptible because the area of opaque structure is continuous and relatively wide.

Stud 3 (1600A; 150 ms) – the most heat was introduced here for the longest time.
The stud is not welded evenly, which is also evidenced by the unevenness of the spatter. This unevenness was reflected in the results achieved. The area where the weld metal with a reduced concentration of Cr and Ni was missing was monitored. The weld metal contains aluminum originating from the tip of the stud. In the place where the weld metal is missing, there are extensive carbides along the grain boundaries and in this area the risk of intergranular corrosion can be expected. Although this strip is not wide (approx. 5 µm), it is unacceptable from the weld metal point of view. At the weld metal TOO interface from the S355 side there is a continuous line of carbides, which will also worsen the corrosion properties and toughness of the joint. Continuous lines of carbides are at the grain boundaries in TOO in S355 steel. This weld is the most critical of the monitored joints, both in terms of the unevenness of the spalls and in terms of the structural condition.

Stud 4 (1400A; 150 ms) – compared to Stud 3, there was a reduced amount of heat, but the same time.
Again, the Stud is not welded perpendicularly to the S355 steel, which was also reflected in the unevenness of the weld bead. There is a significant defect in the weld area, which was created in connection with a large oxide

inclusion that fell out. Its presence was confirmed by EDS analysis and also by morphology. Another globular inclusion of an oxide nature was analyzed in this joint, which, however, was outside the clearly defined area of the weld metal. Its presence documents that a long time and a relatively large heat input caused the melting of a larger part of the S355 steel, which did not mix with the Stud steel and subsequently solidified even with the inclusion present. This is an area of approximately 70 µm in size. This area has a bainitic and sometimes martensitic structure with an increased concentration of chromium, however, its concentration corresponds to the diffusion process, not the process of mixing the melt from the melted Stud. Only at the Stud 4 joint were these small but continuous carbides detected along the austenitic grain boundaries at the Stud location, i.e. on the Wr.N. 1.4541 steel side. Unfortunately, their size does not allow for their separate EDS analysis, but as in the previous case, they are likely to be cementite-based carbides. However, their danger may be not only intergranular corrosion, but also embrittlement of the otherwise tough austenite.

Stud 5 (1400A; 100 ms) – relatively high heat input with shorter mixing time was reflected in the character of the weld metal.
The stud is welded relatively straight, which was positively reflected in the size of the spatter. The mixing of the weld metal melt had, as in Stud 1, areas in which the S355 material was in the middle of the weld metal consisting mainly of Stud, i.e. stainless steel with a reduced concentration of Cr and Ni. at the boundary of the structure – the structure is formed by lower bainite, which passes into upper bainite. No pronounced carbide lines were detected at the interface as in Stud 3. The heterogeneity of the weld metal may represent an increased corrosion risk. The cloudy structure is also not favorable in terms of joint strength, because it can initiate brittle damage.

It is difficult to draw a uniform conclusion from the Stud joints monitored, because in addition to the parameters used, the monitored properties also showed different perpendicularity of their execution. For this reason, more attention was paid to the analyses, so that relevant conclusions could be drawn from a larger amount of data. Of the monitored joints, Stud 2 was the best in terms of structural condition, however, the short time was reflected in the presence of pores and cold joints, therefore it would be appropriate to use a time of 100 ms when using a current of 1600A. The perpendicularity of the Stud welding is decisive.

ČVUT v Praze, Fakulta strojní, Ústav strojírenské technologie, Technická 4, Praha 6, 166 07, Česká republika
T 224 352 628 **E** 12133@fs.cvut.cz **W** u12133.fs.cvut.cz